Report no. 207.
Publication no. 37.

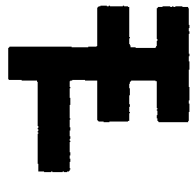

LABORATORIUM VOOR
SCHEEPSBOUWKUNDE

TECHNISCHE HOGESCHOOL DELFT

"CYLINDER MOTIONS IN BEAM WAVES"

by

Ir. J.H. Vugts.

July 1968.

List of figures.

Contents.

List of symbols.

A area of cylinder cross section.

B cylinder width

G centre of gravity

$\overline{GM}$ metacentric height

I polar mass moment of inertia about G of the cylinder in air per unit length

K_w wave exciting moment about G

K'_w wave exciting moment about O

M metacentre

O intersection of watersurface with centre line of cylinder

$\overline{OG}$ vertical position of centre of gravity below the water surface

$Q = \frac{q_{\phi\phi}}{\sqrt{p_{\phi\phi} r_{\phi\phi}}}$ nondimensional damping coefficient of the coupled roll-sway equation.

T cylinder draught

T_ϕ natural roll period by experiment

$Y_w = Y'_w$ horizontal wave exciting force

$Z_w = Z'_w$ vertical wave exciting force

a_{ii} hydrodynamic mass or mass moment of inertia in the i-mode of motion in the Oy'z'-system

a_{ij} mass coupling coefficient in the i-force (moment) equation by motion in the j-mode of the Oy'z'-system

b_{ii} damping coefficient against motion in the i-mode

b_{ij} damping coupling coefficient in the i-force (moment) equation by motion in the j-mode.

c_{ii} hydrostatic restoring coefficient against a displacement in the i-direction

g acceleration of gravity

$k = \frac{2\pi}{\lambda} = \frac{\omega^2}{g}$ wave number

k_ϕ transverse radius of gyration about G of the cylinder in air.

$m=\rho A$ mass of the cylinder section.

p_{ii} coefficient of the mass term in the i-equation

p_{ij} coefficient of the mass coupling term in the i-equation.

q_{ii} coefficient of the damping term in the i-equation

q_{ij} coefficient of the damping coupling term in the i-equation

r_{ii} coefficient of the restoring term in the i-equation

v drift velocity

y_a sway amplitude

z_a heave amplitude

z_e a mean depth under water to consider an effective wave slope

α_w maximum surface wave slope

δ logarithmic decrement of rolling motion

$\varepsilon_{K\zeta}$ phase angle of K'_w with respect to wave elevation at 0

$\varepsilon_{Y\zeta}$ phase angle of Y'_w with respect to wave elevation at 0

$\varepsilon_{Z\zeta}$ phase angle of Z'_w with respect to wave elevation at 0.

$\varepsilon_{y\zeta}$ phase angle of swaying with respect to wave elevation at 0.

$\varepsilon_{z\zeta}$ phase angle of heaving with respect to wave elevation at 0.

$\varepsilon_{\phi\zeta}$ phase angle of rolling with respect to wave elevation at 0.

$\varepsilon_{y\phi}$ phase angle of swaying with respect to rolling

ζ_a wave amplitude

λ wave length

$\nu_\phi = \dfrac{q_{\phi\phi}}{\sqrt{p_{\phi\phi} r_{\phi\phi}}}$ nondimensional roll damping coefficient for pure rolling

ρ specific mass of water

ϕ_a roll amplitude

ω wave frequency

ω_ϕ natural rolling frequency by experiment

$\omega_{res.}$ resonance frequency obtained by prediction b.

Cylinder motions in beam waves.

by

Ir. J.H. Vugts.

Summary.

For the two dimensional case the motion of a body in waves is formulated mathematically. The coupled roll-sway performance is analysed. Coupling coefficients and the vertical position of the centre of gravity play an important role in the ultimate effects. The theoretical predictions are compared with experiments in a small tank.

1. Introduction.

An infinitely long cylinder in beam waves will perform swaying, heaving and rolling motions. The motions are completely determined by the hydrodynamic forces acting on the cylinder and the mass distribution of the rigid body. Both types of quantities can at present be evaluated beforehand, so that a theoretical prediction of the motions is now possible. This will be elaborated in section 2. It will turn out that sway and roll are mutually coupled and that the amount of coupling is strongly dependent on the vertical position of the centre of gravity. To check the correctness of this mathematical model the resulting motions in beam waves were computed and measured for a number of different conditions.

The cylinder used for this investigation has a rectangular cross-section with a rounded bilge. It is studied at two different draughts. In condition 1 the B/T-ratio is 2, in condition 2 it is 4. In both situations the centre of gravity is varied vertically so that in total seven conditions are formed. They are summarized in Table 1. See also figure 1.

Table I: Cylinder conditions.

	Condition 1.				Condition 2.		
	1.1	1.2	1.3	1.4	2.1	2.2	2.3
cylinder length m	0.50				0.50		
beam B m	0.40				0.40		
draught T m	0.20				0.10		
displacement kgf	40				20		
$\overline{KM}$ m	0.1666				0.1833		
$\overline{KG}$ m	0.10	0.12	0.14	0.16	0.10	0.14	0.18
$\overline{OG}$ m	0.10	0.08	0.06	0.04	0	-0.04	-0.08
$\overline{GM}$ m	0.0666	0.0466	0.0266	0.0066	0.0833	0.0433	0.0033
$\overline{GM}/B$ -	0.167	0.117	0.067	0.017	0.208	0.108	0.008
k_ϕ in air m	0.1329				0.1329		
k_ϕ/B -	0.332				0.332		
$r_{\phi\phi} = \rho g A.\overline{GM}$ $\frac{kgf.m}{m}$	5.333	3.733	2.133	0.533	3.333	1.733	0.1333

The experiments were carried out in a small tank of ca. 15 m. length with a wetted cross-section of 0.50 x 0.55 m^2. The wave-maker generated waves of a constant amplitude of 0.01 m. It is clear that for the longer wave-periods the experiments were influenced by the restricted waterdepth and possibly by the reflection of waves which were not fully damped out at the beaches. The restricted waterdepth can approximately be accounted for in the prediction of swaying and heaving, as will be shown. Apart from the indirect effect via coupling with swaying the waterdepth has little direct influence on rolling. The results of the experiments can therefore be used satisfactorily to compare with the predictions, which are based on deep water coefficients.

The motions will also be analysed for the influence of the coupling coefficients and for the effect of the vertical position of the centre of gravity.

2. The theoretical prediction of the motions.

The equations of motion of the cylindrical body are expressed by:

$$\left.\begin{aligned} m\ddot{y} &= Y \\ m\ddot{z} &= Z \\ I\ddot{\phi} &= K \end{aligned}\right\} \quad (1)$$

The coordinate system Gyz is shown in figure 1.
The right hand sides of these equations are composed of the hydrodynamic forces due to the oscillations of the body and to the incoming waves.
As the hydrodynamic forces have nothing to do with rigid body characteristics they are best expressed in the Oy'z'-system, which is independent of the position of G. In a formal description of the linear forces, with subsequently a simple reduction by hydrostatics and by symmetry considerations, they can be expressed as:

$$\left.\begin{aligned} Y' &= -a_{yy}\ddot{y}'-b_{yy}\dot{y}'-a_{y\phi}\ddot{\phi}'-b_{y\phi}\dot{\phi}'+Y_w' \\ Z' &= -a_{zz}\ddot{z}'-b_{zz}\dot{z}'-c_{zz}z'+Z_w' \\ K' &= -a_{\phi\phi}\ddot{\phi}'-b_{\phi\phi}\dot{\phi}'-c_{\phi\phi}\phi'-a_{\phi y}\ddot{y}'-b_{\phi y}\dot{y}'+K_w' \end{aligned}\right\} \quad (2)$$

Transformation from Oy'z' to Gyz is obtained by:

$$\left.\begin{aligned} y &= y' - \overline{OG}.\phi' \\ z &= z' \\ \phi &= \phi' \\ Y &= Y';\ Y_w = Y_w' \\ Z &= Z';\ Z_w = Z_w' \\ K &= K'+\overline{OG}.Y';\ K_w = K_w'+\overline{OG}.Y_w' \end{aligned}\right\} \quad (3)$$

Substituting the ultimate result in (1) and rearranging the terms gives:

$$\left.\begin{aligned} p_{yy}\ddot{y}+q_{yy}\dot{y}+ \quad p_{y\phi}\ddot{\phi}+q_{y\phi}\dot{\phi} &= Y_w \\ p_{\phi\phi}\ddot{\phi}+q_{\phi\phi}\dot{\phi}+r_{\phi\phi}\phi+p_{\phi y}\ddot{y}+q_{\phi y}\dot{y} &= K'_w+\overline{OG}.Y'_w \\ p_{zz}\ddot{z}+q_{zz}\dot{z}+r_{zz}z &= Z_w \end{aligned}\right\} \quad (4)$$

where:

$$\left.\begin{aligned} p_{yy} &= m+a_{yy} = \rho A+a_{yy} \\ q_{yy} &= b_{yy} \\ p_{y\phi} &= a_{y\phi}+\overline{OG}.a_{yy} \\ q_{y\phi} &= b_{y\phi}+\overline{OG}.b_{yy} \\ p_{\phi\phi} &= I+a_{\phi\phi}+\overline{OG}.a_{\phi y}+\overline{OG}^2.a_{yy}+\overline{OG}.a_{y\phi} \\ q_{\phi\phi} &= b_{\phi\phi}+\overline{OG}.b_{\phi y}+\overline{OG}^2.b_{yy}+\overline{OG}.b_{y\phi} \\ r_{\phi\phi} &= c_{\phi\phi}+\overline{OG}.\rho gA = \rho gA.\overline{GM}. \\ p_{\phi y} &= a_{\phi y}+\overline{OG}.a_{yy} \\ q_{\phi y} &= b_{\phi y}+\overline{OG}.b_{yy} \\ p_{zz} &= m+a_{zz} = \rho A+a_{zz} \\ q_{zz} &= b_{zz} \\ r_{zz} &= c_{zz} = \rho gB. \end{aligned}\right\} \quad (5)$$

$$\left.\begin{aligned} Y'_w &= Y_w = Y'_a \sin(\omega t+\varepsilon_{Y\zeta}) \\ Z'_w &= Z_w = Z'_a \sin(\omega t+\varepsilon_{Z\zeta}) \\ K'_w &= K'_a \sin(\omega t+\varepsilon_{K\zeta}) \end{aligned}\right\} \quad (5)$$

The same practice as outlined above has been followed by Tasai to formulate the motion problem of a ship model in beam seas [1].

All of the coefficients and the wave exciting forces in (4) can be computed theoretically with good accuracy. This has been proved in [2], where computations have been compared with experiments over a large range of frequencies for (among other forms) the same sections as used here. The one important exception is the roll damping coefficient $b_{\phi\phi}$. Viscous contributions in the roll damping are distinctly present and because of their importance they must be accounted for. Therefore roll extinction experiments have been done to provide an experimental value for $q_{\phi\phi}$. It will be seen that even very large variations in roll damping will only effect the motion responses in the usually very narrow range of roll resonance. Since all other quantities are obtained with sufficient accuracy by direct computations from theoretical hydrodynamics assuming an ideal fluid the motion predictions are essentially of a truly theoretical nature.

From (5) it is obvious that the vertical position of G may play an important role in the coupled sway-roll performance. The influence of coupling may be quite different for different distributions of the loading, that is for different values of $\overline{OG}$ and I, while all coefficients a_{ij}, b_{ij} and c_{ij}, remain essentially constant as long as the draught does not change. In the programme under consideration I has also been kept constant, so that $\overline{OG}$ is the only variable.

The computations have been carried out for four cases:

a) using only theoretical values for all of the quantities in the equations (4) and (5);

the value of the hydrodynamic quantities a_{ij}, b_{ij}, Y'_a, Z'_a, K'_a and $\varepsilon_{Z\zeta}$ is given in ref [2]; unfortunately the $\varepsilon_{Y\zeta}$ is in error there, it must be inverted with respect to -90 degrees; $\varepsilon_{K\zeta} = \varepsilon_{Y\zeta}$ when M is above 0, $\varepsilon_{K\zeta} = \varepsilon_{Y\zeta} + 180^{o}$ when M is below 0;

b) as above, but with an increased roll damping, so that $q_{\phi\phi}$ is equal to the measured roll damping at the natural frequency of oscillation in an extinction experiment; for other frequencies the increase is kept constant; the selection of the value of $q_{\phi\phi}$ is described in section 3;

c) as in b), but with $a_{y\phi} = a_{\phi y} = b_{y\phi} = b_{\phi y} = 0$; this does not mean that all coupling terms are zero, as $p_{y\phi} = p_{\phi y}$ and $q_{y\phi} = q_{\phi y}$ do not vanish because of the distance $\overline{OG}$;

d) according to the equation

$$\frac{\ddot{\phi}}{\omega_\phi^2} + \frac{\nu_\phi}{\omega_\phi}\dot{\phi} + \phi = \alpha_w e^{-kz_e} , \qquad (6)$$

presenting the usual formulation of pure rolling in beam waves; ω_ϕ and ν_ϕ are taken from the extinction experiments; z_e is taken equal to $\frac{1}{2}T$.

3. Extinction experiments in roll and their analysis.

The extinction experiments were done with the model located in the middle of the tank length and/or with the model close to the beach. The results show large differences, as will be seen. Assuming that the induced swaying can be neglected (y=0) the test is described by equation (4) with $Y'_w = K'_w = 0$:

$$p_{\phi\phi}\ddot{\phi} + q_{\phi\phi}\dot{\phi} + r_{\phi\phi}\phi = 0. \qquad (7)$$

In (7) $r_{\phi\phi}$ is known: $r_{\phi\phi} = \rho g A.\overline{GM}$, while $p_{\phi\phi}$ can be approximated satisfactorily by measuring the natural period. Then $q_{\phi\phi}$ can be solved by recording the roll angle ϕ.

The natural period of the rolling is found to be:

$$T_\phi = \frac{4\pi\, p_{\phi\phi}}{\sqrt{4p_{\phi\phi} r_{\phi\phi} - q_{\phi\phi}^2}} \tag{8}$$

For lightly damped oscillations (very small $q_{\phi\phi}$ compared to the product $p_{\phi\phi}\ r_{\phi\phi}$) this results for $p_{\phi\phi}$ in:

$$p_{\phi\phi} \cong \frac{r_{\phi\phi} T_\phi^2}{4\pi^2} \tag{9}$$

From (5) it turns out that $p_{\phi\phi}$ is composed of many different contributions in which I, the massmoment of inertia in air, will generally dominate the other terms. Yet (9) is thought to be a better approximation than $p_{\phi\phi} \cong I$, because it automatically takes into account the influence of the vertical position of G. Furthermore the relation (9) is much more practical since it is not easy to determine I.
The damping coefficient $q_{\phi\phi}$ is determined by the decrease of the oscillations, see figure 2. Putting:

$$\delta = -\frac{q_{\phi\phi}}{2p_{\phi\phi}} T_\phi = \ln\phi_B - \ln\phi_A \tag{10}$$

there results:

$$q_{\phi\phi} = \left[\frac{r_{\phi\phi} p_{\phi\phi} \delta^2}{\pi^2 + \frac{1}{4}\delta^2}\right]^{\frac{1}{2}} \tag{11}$$

The measured T_ϕ and the experimental $q_{\phi\phi}$ are presented in figure 3 for condition 1 and in figure 4 for condition 2. For comparison the $b_{\phi\phi}$ and $q_{\phi\phi}$ given by potential theory are also indicated in the figures.

It is to be expected that the actual roll damping during the tests is appreciably higher than a theoretical estimate because of the friction of the water film between the end bulkheads of the cylinder and the tank walls. The extinction experiments taken near the beach of the tank do not exhibit this tendency in figure 3. The curve B drawn through the 4 measured points intersects the theoretical $q_{\phi\phi}$-curve C. This must be due to reflection effects, but it can not be explained further.

Unfortunately this fact was only established after the tests, while only 2 experiments in the middle of the tank length were available. The ultimate $q_{\phi\phi}$ -curve A, used in the motion predictions, is drawn through these two points and its trend has been adapted to curve B. Curve A does not intersect the theoretical curve C.
For condition 2 the same philosophy has been applied in figure 4. Here even less measurements were available, so that the $q_{\phi\phi}$ -values are of a somewhat disputable nature. However, this has no serious consequences for the motion predictions.
It is remarkable that the mutual order of magnitude of the curves A and B in figure 4 is contrary to that in figure 3. An explanation cannot be given.

4. Experiments in waves.

4.1. The experimental set-up.

A sketch of the experimental facility is shown in figure 5.
The wave generator is of the flap type. During the tests the point of rotation of the flap was at the tank bottom. The wave periods were varied between 0.5 sec. and 2.4 sec. The wave height was kept constant at 0.02 m from crest to trough. The wave maker setting was determined before the actual tests without the model in the tank. The stated waves are therefore the undisturbed, incoming waves. However, it is possible that deviations from the nominal wave height occur since the generated waves will not be reproduced exactly.
The rolling was measured by a gyro installed in the cylinder. The accuracy of the measurements is approximately $\pm$ 0.2 degrees.
For swaying a vertical rod was installed which hinged at the centre of gravity. It was connected to a very light cross which was guided horizontally. The motion of the cross was measured by a potentiometer; see figure 5. The accuracy of this set-up is about $\pm$ 0.2 x 10^{-3} m.
Both roll angle and sway motion were recorded at a UV-recorder. The recordings showed a stationary part of sufficient length so that transient phenomena and later reflection and interference effects could be separated distinctly from the desired information.

Said parts of the recordings were analysed manually to obtain the roll angle ϕ_a, sway amplitude y_a, the phase difference of sway with respect to roll $\varepsilon_{y\phi}$ and the drift velocity v. A typical example of a recording is reproduced in figure 6.

4.2. The results of experiments and predictions.

The predicted heaving and its phase with respect to the wave motion at G is given in the figures 7 and 8. Heaving was not measured. By the finite water depth the motion of the water particles in the waves is deformed from a circle to an ellipse. The dotted line in the heave prediction is obtained by multiplication with the ratio (short axis ellipse at finite waterdepth) / (diameter circle at infinite depth). The ratio has been determined at a depth of the half draught of the section. This supposes that the dynamic performance of the cylinder can be separated from the static response and that the former is essentially unchanged. This seems a reasonable hypothesis for a first approximation.

The various $q_{\phi\phi}$ - values used in the predictions a, b and c of section 2 are summarized in the figures A1 and A7 at the end of the paper. It is clear that the effect of the coupling coefficient $b_{\phi y}$ has a very great influence on $q_{\phi\phi}$ and can not be neglected; compare the curves marked b and c, respectively.

The difference in the exciting moment used in the predictions a, b and c on the one hand and the Froude-Krylov moment in prediction d on the other hand is illustrated in the figures A2 and A8. It shows that the Froude-Krylov hypothesis is not a satisfactory base to compute the rolling moment.

The experimental results for rolling and swaying in condition 1 are presented in the figures A3 through A6. The four predictions according to section 2 are shown as well. The best theoretical prediction (curve b) for swaying has been multiplied with the ratio (long axis ellipse at finite waterdepth)/(diameter circle at infinite depth) to account for the restricted waterdepth, just as in heaving.

The same information for condition 2 is given in the figures A9 through A11.

An analogous correction for shallow water effects has been applied to swaying.

The measured drift velocities of both conditions have been plotted in figure A15 and A16.

5. Discussion of the results.

The theoretical predictions, which are fundamentally most correct, are the curves marked b. The agreement between those curves and the experiments is generally very satisfactory. That the top of the roll resonance is lower or higher than the experiments is a direct consequence of the chosen value of $q_{\phi\phi}$, which could not be established very accurately, as discussed in section 3. The shift of the theoretical resonance zone with respect to the experimental resonance is of more fundamental interest, since it does not depend on $q_{\phi\phi}$. Yet it is not of great importance, considering the state of the art and possible practical applications. That the mathematical model is basically correct, is indicated clearly by the dip in the sway-curve and by the phase-relation $\varepsilon_{y\phi}$. The measurements of $\varepsilon_{y\phi}$ show an unexpected jump of about 180 degrees in some conditions, which is also predicted by the computations.

The completely theoretical curves marked a nearly coincide with the curves b, except for a narrow range about roll resonance. The increased roll damping lowers the ϕ_a-prediction, smooths the coupling effects of roll into sway and flattens the phase difference, but leaves the predictions further unchanged.

The same cannot be said about the curves marked c. It is clearly not a matter of accuracy but of the utmost importance to take due account of the coupling coefficients $a_{\phi y} = a_{y\phi}$ and $b_{\phi y} = b_{y\phi}$. This is most clearly demonstrated by the phase difference $\varepsilon_{y\phi}$, where the c-curves are distinctly in error. The greater the distance $\overline{OG}$ (positive for condition 1, or negative for condition 2) the greater their influence.

The predictions d, obtained by the familiar equation (6) for pure rolling in beam waves, differ in one case only slightly from the experiments (e.g. condition 1.2), in another case greatly. The general tendency of the coupling effects with swaying is to lower and to narrow the roll response, especially at the high frequency side. This can easily be shown by vector diagrams of the left hand side of the roll equation of motion, using the computed $\varepsilon_{y\phi}$. This effect is paricularly seen in condition 2.1 and 2.2. The phase lag $\varepsilon_{y\phi}$ does, of course, not show a jump of approximately 180 degrees as the predictions a and b and the experiments do in the conditions 1.4, 2.2 and 2.3. That the method d is not to be recommended for general use is also illustrated by condition 2.1. Here $\overline{OG} = 0$ so that for $a_{\phi y} = a_{y\phi} = b_{\phi y} = b_{y\phi} = 0$ rolling and swaying are fully decoupled. In principle now method c and d are equal, except for the precise value of $p_{\phi\phi}$ and $q_{\phi\phi}$ and determination of the exciting moment. These moments differ greatly, as is shown in figure A8. As a consequence the roll responses c and d differ also greatly; figure A9.

The exciting moment about G is composed of the hydrodynamic moment about O and the sway force:

$$K_w = K'_w + \overline{OG}.Y'_w.$$

K'_w and Y'_w are either in phase or in counterphase depending on the position of the metacentre M with respect to O. The distance $\overline{OG}$ may be positive or negative. Therefore K_w may become zero for a certain wave frequency and change in phase. This is shown in condition 2.2 at ω=4.55 sec^{-1}. In the conditions 1.4 and 2.3 the phase of K_w is contrary to that of the other conditions 1 and 2, respectively, for all frequencies.

It appears that the influence of shallow water on swaying can be accounted for reasonably by multiplication of the response with the ratio (long axis ellipse)/ (diameter circle), given by the motion of the water particles in the wave at restricted and infinite depth. The experimental scatter is no doubt a consequence of wave reflection and subsequent interference effects, which were present for waves with periods longer

than 1.5 sec. In the very low frequency range the measured roll angles generally show a slight hump. This must be attributed to a stronger coupling with swaying in the experiments by the much larger y_a's than predicted. However, it is of no practical importance.

Finally the theoretical results marked b for condition 1 and for condition 2 have been plotted non-dimensionally in figure A12 en A13, using $\overline{GM}/B$ as a parameter. The base of these figures is $\omega/\omega_{res.}$, where $\omega_{res.}$ is the frequency where the largest ϕ_a is found in the respective curves labelled b. The figures exhibit some interesting features. Rolling is a typical resonance phenomenon. When plotted on the basis of tuning factor the curves nearly coincide. There is a very narrow peak, which has a slight tendency to become somewhat broader when the $\overline{GM}$ decreases. Little can be said about the maximum magnification factor for the various conditions 1 or 2 separately. But for condition 1 as a whole it is roughly twice as large as for condition 2. This is not explained by the nondimensional damping coefficients $Q = q_{\phi\phi}/\sqrt{p_{\phi\phi} r_{\phi\phi}}$ which have been plotted in fig. A14. Q is equivalent to ν_ϕ for the one degree of freedom rolling. But contrary to ν_ϕ Q does not solely control the rolling at resonance by the coupling effects.
Swaying on the other hand is an absolute phenomenon mainly dependent on the waves. Plotted on wave frequency the curves for the various conditions 1 practically coincide (fig.A3-A6), just as for the conditions 2 (fig.A9-A11).
Only at roll resonance there is a different performance by coupling. On a basis of roll tuning factor the various sway curves are distinctly different (fig.A12 and A13). The influence of the coupling effects, causing the hump and hollow in the sway curves, decreases strongly, when $\overline{GM}$ decreases. Both the magnitude and the width of the influenced range become less.

The phase difference $\varepsilon_{y\phi}$ is a relative quantity, just as rolling. For condition 1 $\varepsilon_{y\phi}$ varies somewhat with $\overline{GM}/B$, for condition 2 hardly any difference can be noticed.

During the tests the drift velocities have been measured. The fact that there is a drift velocity shows that apart from the oscillatory lateral force a mean component must be present. No attempt has been made to predict or to analyse this effect, but the experimental results are shown in the figures A15 and A16. It is not impossible that especially these secondary effects are strongly influenced by the test circumstances as the way of generating waves and the dimensions of the tank. So the information must be handled carefully.

6. Conclusions.

1. The experiments show that the mathematical model of section 2 is fundamentally correct. Roll and sway are coupled by comprehensive coefficients made up of the actual coupling coefficients $a_{\phi y}$ and $b_{\phi y}$, of the hydrodynamic sway coefficients a_{yy} and b_{yy} and of the vertical position of the centre of gravity $\overline{OG}$.

2. Taking account of the coupling coefficients $a_{\phi y}$ and $b_{\phi y}$ is not a matter of improving the accuracy, but of primary importance for the mathematical model to exhibit the essential characteristics of the phenomena. Compare the curves labelled b and c in the figures A3-A6 and A9-A11.

3. Increasing the roll damping does not introduce any new aspect in the motions; it solely lowers the peak value in rolling, flattens the hump and hollow in the sway-curve at roll resonance and makes the phase transition less steep. See the curves a and b in the figures A3-A6 and A9-A11.

4. In general the Froude-Krylov moment can not be considered as a sound base for the excitation in rolling. See figure A2 and A8. The actual moment is not only dependent on the metacentric height, so on the relative position of G and M, but also on the absolute position of G and M with respect to the water surface.

5. The one degree of freedom prediction (curves d in the figures A3-A6 and A9-A11) sometimes offers reasonable results, sometimes the results are poor. It is better to use an advanced method of prediction, which takes account of the important variables.

6. The influence of the coupling of roll into sway is not large; see figure A12 and A13. The influence still decreases for diminishing $\overline{GM}$. The influence of the coupling of sway into roll can not be estimated beforehand. It will depend on the shape of the section, the condition of loading and the vertical position of the centre of gravity. So it may be quite different in different cases. The general tendency is to lower and to narrow the roll response, especially at the high frequency side.

7. For the various sub-conditions the relative roll response is very similar, both to magnitude and phase, despite the large differences in $\overline{GM}/B$. See figure A12 and A13.

8. The shallow water effect on swaying is very reasonably accounted for by multiplication of the deep water response with the ratio (long axis ellipse)/(diameter circle) of the track of the water particles in the wave.

Acknowledgement.

The experiments described in this report have been carried out for the author by the American students O.H. Oakley of M.I.T. and P.B. Fontneau of Webb Institute in July 1967, during their stay at the Shipbuilding Laboratory as student-trainees.
The author expresses his sincere gratitude for their work.

References.

[1] Tasai, F., "Ship motions in beam seas"; Reports of Research Institute for Applied Mechanics, vol.XIII, No. 45, 1965.

[2] Vugts, J.H., "The hydrodynamic coefficients for swaying, heaving and rolling cylinders in a free surface"; Netherlands Ship Research Centre TNO, Report 112S, May 1968.

REPORT No. 115 S
(S 2/–)

December 1968

NEDERLANDS SCHEEPSSTUDIECENTRUM TNO
NETHERLANDS SHIP RESEARCH CENTRE TNO
SHIPBUILDING DEPARTMENT LEEGHWATERSTRAAT 5, DELFT

★

CYLINDER MOTIONS IN BEAM WAVES

(BEWEGINGEN VAN CILINDERS IN DWARSINKOMENDE GOLVEN)

by

IR. J. H. VUGTS
(Shipbuilding Laboratory, Delft University of Technology)

Issued by the Council

VOORWOORD

Dit rapport is het tweede dat voortvloeit uit het uitgebreide researchprogramma, onderhanden bij het Laboratorium voor Scheepsbouwkunde van de Technische Hogeschool te Delft en dat tot doel heeft het verifiëren van een theoretische methode voor het bepalen van scheepsbewegingen.

Eerder in 1968 verscheen rapport no. 112 S „De hydrodynamische coëfficiënten voor het verzetten, dompen en slingeren van cilinders in een vrije vloeistof oppervlakte" van dezelfde auteur. In deze publikatie zijn de coëfficiënten die de grondelementen vormen voor het bepalen van de scheepsbewegingen berekend met de potentiaaltheorie en gecontroleerd door proeven met een aantal cilindrische lichamen. De overeenkomst bleek bevredigend en de werkzaamheden zullen worden voortgezet met werkelijke, driedimensionale, scheepsmodellen.

In dit tweede rapport zijn de resultaten toegepast op de bewegingen van een oneindig lange cilindervorm in dwarsinkomende golven teneinde de slingerbeweging en de koppeling daarvan met verzetten te analyseren. Door de theoretisch bepaalde bewegingen te vergelijken met de resultaten van metingen voor een vrij rijvend cilindermodel wordt geverifieerd of het mathematisch model de fysische realiteit dekt.

De slinger-verzet beweging verdient speciale aandacht omdat de koppel-coëfficiënten en de plaats van het zwaartepunt ten opzichte van de waterlijn van groot belang zijn. Bij slingerresonantie spelen ook visceuze effecten een grote rol.

Uit de resultaten blijkt onder andere dat het beschouwen van zuiver slingeren tot niet te verwaarlozen fouten kan leiden en dat hetzelfde geldt voor het toepassen van de veel gebruikte Froude-Krylov hypothese voor het door golven opgewekte moment. Voor een betrouwbare prognose wordt aanbevolen om een methode toe te passen die de koppeling en de invloed van de plaats van het zwaartepunt verdisconteert.

HET NEDERLANDS SCHEEPSSTUDIECENTRUM TNO

PREFACE

This report is the second one resulting from the extensive research programme that is being carried out by the Shipbuilding Laboratory of the Delft University of Technology and that aims at a verification of a theoretical approach for the prediction of ship motions.

Earlier in 1968, report no. 112 S "The hydrodynamic coefficients for swaying, heaving and rolling cylinders in a free surface" by the same author, was published. In this publication the coefficients which form the basic elements for the ship motion prediction were computed with the potential theory and checked by experiments with a number of cylindrical shapes. The agreement proved to be satisfactory and the work will proceed with actual, threedimensional, shipmodels.

In this second report the results have been applied to the motions of an infinitely long cylinder in beam waves to analyse the rolling motion and its coupling with swaying. By comparing the theoretically predicted motions with the results of measurements for a freely floating cylinder model, it is verified whether the mathematical model covers the physical reality.

The roll-sway motion deserves special attention as the coupling coefficients and the position of the centre of gravity with respect to the waterline are of great importance. At roll resonance viscous effects play an important role as well.

From the results it appears, among other things, that considering only pure rolling may lead to unnegligible errors and that the often used Froude-Krylov hypothesis for the moment excited by waves may have a similar effect. For a reliable prediction it is recommended to use a method which includes coupling and the influence of the position of the centre of gravity.

THE NETHERLANDS SHIP RESEARCH CENTRE TNO

CONTENTS

LIST OF SYMBOLS

A Area of cylinder cross section

B Cylinder width

G Centre of gravity

$\overline{GM}$ Metacentric height

I Polar mass moment of inertia about G of the cylinder in air per unit length

K_w Wave exciting moment about G

K'_w Wave exciting moment about O

M Metacentre

O Intersection of watersurface with centre line of cylinder

$\overline{OG}$ Vertical position of centre of gravity below the water surface

$Q = \frac{q_{\phi\phi}}{\sqrt{p_{\phi\phi} r_{\phi\phi}}}$ Nondimensional damping coefficient of the coupled roll-sway equation

T Cylinder draught

T_ϕ Natural roll period by experiment

$Y_w = Y'_w$ Horizontal wave exciting force

$Z_w = Z'_w$ Vertical wave exciting force

a_{ii} Hydrodynamic mass or mass moment of inertia in the i-mode of motion in the $Oy'z'$-system

a_{ij} Mass coupling coefficient in the i-force (moment) equation by motion in the j-mode of the $Oy'z'$-system

b_{ii} Damping coefficient against motion in the i-mode

b_{ij} Damping coupling coefficient in the i-force (moment) equation by motion in the j-mode

c_{ii} Hydrostatic restoring coefficient against a displacement in the i-direction

g Acceleration of gravity

$k = \frac{2\pi}{\lambda} = \frac{\omega^2}{g}$ Wave number

k_ϕ Transverse radius of gyration about G of the cylinder in air

$m = \varrho A$ Mass of the cylinder per unit length

p_{ii} Coefficient of the mass term in the i-equation

p_{ij} Coefficient of the mass coupling term in the i-equation

q_{ii} Coefficient of the damping term in the i-equation

q_{ij} Coefficient of the damping coupling term in the i-equation

r_{ii} Coefficient of the restoring term in the i-equation

v Drift velocity

y_a Sway amplitude

z_a Heave amplitude

z_e A mean depth under water to consider an effective wave slope

α_w Maximum surface wave slope

δ Logarithmic decrement of rolling motion

$\varepsilon_{K\zeta}$ Phase angle of K_w' with respect to wave elevation at O

$\varepsilon_{Y\zeta}$ Phase angle of Y_w' with respect to wave elevation at O

$\varepsilon_{Z\zeta}$ Phase angle of Z_w' with respect to wave elevation at O

$\varepsilon_{y\zeta}$ Phase angle of swaying with respect to wave elevation at O

$\varepsilon_{z\zeta}$ Phase angle of heaving with respect to wave elevation at O

$\varepsilon_{\phi\zeta}$ Phase angle of rolling with respect to wave elevation at O

$\varepsilon_{y\phi}$ Phase angle of swaying with respect to rolling

ζ_a Wave amplitude

λ Wave length

$\nu_\phi = \frac{q_{\phi\phi}}{\sqrt{p_{\phi\phi} r_{\phi\phi}}}$ Nondimensional roll damping coefficient for pure rolling

ϱ Specific mass of water

ϕ_a Roll amplitude

ω Wave frequency

ω_ϕ Natural rolling frequency by experiment

ω_{res} Resonance frequency obtained by prediction b (see section 2)

CYLINDER MOTIONS IN BEAM WAVES*

by

Ir. J. H. VUGTS

Summary

For the two-dimensional case the motion of a body in waves is formulated mathematically. The coupled roll-sway performance is analysed. Coupling coefficients and the vertical position of the centre of gravity play an important role in the ultimate effects. The theoretical predictions are compared with experiments in a small tank.

1 Introduction

An infinitely long cylinder in beam waves will perform swaying, heaving and rolling motions. The motions are completely determined by the hydrodynamic forces acting on the cylinder and the mass distribution of the rigid body. Both types of quantities can at present be evaluated beforehand, so that a theoretical prediction of the motions is now possible. This will be elaborated in section 2. It will turn out that sway and roll are mutually coupled and that the amount of coupling is strongly dependent on the vertical position of the centre of gravity. To check the correctness of this mathematical model the resulting motions in beam waves were computed and measured for a number of different conditions.

The cylinder used for this investigation has a rectangular cross section with a rounded bilge. It is studied at two different draughts. In condition 1 the B/T-ratio is 2, in condition 2 it is 4. In both situations the centre of gravity is varied vertically so that in total seven conditions are formed. They are summarized in Table I. See also figure 1.

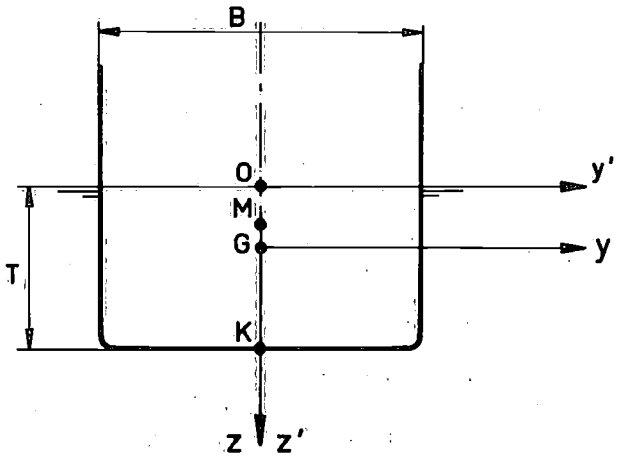

Fig. 1. System of coordinates

* Publication no. 37 of the Shipbuilding Laboratory of the Delft University of Technology.

Table I: Cylinder conditions

		Condition 1				Condition 2		
		1.1	1.2	1.3	1.4	2.1	2.2	2.3
cylinder length	m	0.50				0.50		
breadth B	m	0.40				0.40		
draught T	m	0.20				0.10		
displacement	kgf	40				20		
$\overline{KM}$	m	0.1666				0.1833		
$\overline{KG}$	m	0.10	0.12	0.14	0.16	0.10	0.14	0.18
$\overline{OG}$	m	0.10	0.08	0.06	0.04	0	−0.04	−0.08
$\overline{GM}$	m	0.0666	0.0466	0.0266	0.0066	0.0833	0.0433	0.0033
$\overline{GM}/B$	–	0.167	0.117	0.067	0.017	0.208	0.108	0.008
k_ϕ in air	m	0.1329				0.1329		
k_ϕ/B	–	0.332				0.332		
$r_{\phi\phi} = \varrho g A \cdot \overline{GM}$	kgf·m/m	5.333	3.733	2.133	0.533	3.333	1.733	0.1333

The experiments were carried out in a small tank of ca. 15 m length with a wetted cross section of 0.50×0.55 m^2. The wave maker generated waves of a constant amplitude of 0.01 m. It is clear that for the longer wave periods the experiments were influenced by the restricted waterdepth and possibly by the reflection of waves which were not fully damped out at the beaches. The restricted waterdepth can approximately be accounted for in the prediction of swaying and heaving, as will be shown. Apart from the indirect effect via coupling with swaying the waterdepth has little direct influence on rolling. The results of the experiments can therefore be used satisfactorily to be compared with the predictions, which are based on deep water coefficients.

The motions will also be analysed for the influence of the coupling coefficients and for the effect of the vertical position of the centre of gravity.

2 The theoretical prediction of the motions

The equations of motion of the cylindrical body are expressed by

$$\left.\begin{aligned} m\ddot{y} &= Y \\ m\ddot{z} &= Z \\ I\ddot{\phi} &= K \end{aligned}\right\} \quad (1)$$

The coordinate system Gyz is shown in figure 1. The right hand sides of these equations are composed of the hydrodynamic forces due to the oscillations of the body and to the incoming waves. As the hydrodynamic forces have nothing to do with rigid body characteristics they are best expressed in the $Oy'z'$-system, which is independent of the position of G (see figure 1). In a formal description of the linear forces, with subsequently a simple reduction by hydrostatics and by symmetry considerations as discussed in [2], they can be expressed as

$$\left.\begin{aligned} Y' &= -a_{yy}\ddot{y}' - b_{yy}\dot{y}' - a_{y\phi}\ddot{\phi}' - b_{y\phi}\dot{\phi}' + Y'_w \\ Z' &= -a_{zz}\ddot{z}' - b_{zz}\dot{z}' - c_{zz}z' + Z'_w \\ K' &= -a_{\phi\phi}\ddot{\phi}' - b_{\phi\phi}\dot{\phi}' - c_{\phi\phi}\phi' - a_{\phi y}\ddot{y}' - b_{\phi y}\dot{y}' + K'_w \end{aligned}\right\} \quad (2)$$

Transformation from $Oy'z'$ to Gyz is obtained by

$$\left.\begin{aligned} y &= y' - \overline{OG}\cdot\phi' \\ z &= z' \\ \phi &= \phi' \\ Y &= Y';\ Y_w = Y'_w \\ Z &= Z';\ Z_w = Z'_w \\ K &= K' + \overline{OG}\cdot Y';\ K_w = K'_w + \overline{OG}\cdot Y'_w \end{aligned}\right\} \quad (3)$$

Substituting the ultimate result in equations (1) and rearranging the terms gives

$$\left.\begin{aligned} &p_{yy}\ddot{y} + q_{yy}\dot{y} + p_{y\phi}\ddot{\phi} + q_{y\phi}\dot{\phi} = Y_w \\ &p_{\phi\phi}\ddot{\phi} + q_{\phi\phi}\dot{\phi} + r_{\phi\phi}\phi + p_{\phi y}\ddot{y} + q_{\phi y}\dot{y} = K'_w + \overline{OG}\cdot Y'_w \\ &p_{zz}\ddot{z} + q_{zz}\dot{z} + r_{zz}z = Z_w \end{aligned}\right\} \quad (4)$$

where

$$\left.\begin{aligned} p_{yy} &= m + a_{yy} = \varrho A + a_{yy} \\ q_{yy} &= b_{yy} \\ p_{y\phi} &= a_{y\phi} + \overline{OG}\cdot a_{yy} \\ q_{y\phi} &= b_{y\phi} + \overline{OG}\cdot b_{yy} \\ p_{\phi\phi} &= I + a_{\phi\phi} + \overline{OG}\cdot a_{\phi y} + \overline{OG}^2\cdot a_{yy} + \overline{OG}\cdot a_{y\phi} \\ q_{\phi\phi} &= b_{\phi\phi} + \overline{OG}\cdot b_{\phi y} + \overline{OG}^2\cdot b_{yy} + \overline{OG}\cdot b_{y\phi} \\ r_{\phi\phi} &= c_{\phi\phi} + \overline{OG}\cdot\varrho g A = \varrho g A\cdot\overline{GM} \\ p_{\phi y} &= a_{\phi y} + \overline{OG}\cdot a_{yy} \\ q_{\phi y} &= b_{\phi y} + \overline{OG}\cdot b_{yy} \\ p_{zz} &= m + a_{zz} = \varrho A + a_{zz} \\ q_{zz} &= b_{zz} \\ r_{zz} &= c_{zz} = \varrho g B \\ Y'_w &= Y_w = Y'_a \sin(\omega t + \varepsilon_{Y\zeta}) \\ Z'_w &= Z_w = Z'_a \sin(\omega t + \varepsilon_{Z\zeta}) \\ K'_w &= K'_a \sin(\omega t + \varepsilon_{K\zeta}) \end{aligned}\right\} \quad (5)$$

The same practice as outlined above has been followed by Tasai to formulate the motion problem of a ship model in beam seas [1].

All the coefficients and the wave-exciting forces in equation (4) can be computed theoretically with good accuracy by potential theory. This has been proved in [2], where computations have been compared with experiments over a large range of frequencies for (among other forms) the same sections as used here. The one important exception is the roll damping coefficient $b_{\phi\phi}$. Viscous contributions in the roll damping are distinctly present and because of their importance they must be accounted for. Therefore roll extinction experiments have been done to provide an experimental value for $q_{\phi\phi}$. It will be seen that even very large variations in roll damping will only effect the motion responses in the usually very narrow range of roll resonance. Since all other quantities are obtained with sufficient accuracy by direct computations from theoretical hydrodynamics, an ideal fluid being assumed, the motion predictions are essentially of a truly theoretical nature.

From equations (5) it is obvious that the vertical position of G may play an important role in the coupled sway-roll performance. The influence of coupling may be quite different for different distributions of the loading, that is for different values of $\overline{OG}$ and I, while all coefficients a_{ij}, b_{ij} and c_{ij} remain essentially constant as long as the draught does not change. In the programme under consideration I has also been kept constant, so that $\overline{OG}$ is the only variable.

The computations have been carried out for four cases

a. using only theoretical values for all of the quantities in the equations (4) and (5);
the value of the hydrodynamic quantities a_{ij}, b_{ij}, Y_a', Z_a', K_a' and $\varepsilon_{Z\zeta}$ is given in ref. [2]; unfortunately the $\varepsilon_{Y\zeta}$ in figures 11.1–11.5 is in error there, it must be inverted with respect to -90 degrees; $\varepsilon_{K\zeta} = \varepsilon_{Y\zeta}$ when M is above O, $\varepsilon_{K\zeta} = \varepsilon_{Y\zeta} + 180°$ when M is below O;

b. as above, but with an increased roll damping, so that $q_{\phi\phi}$ is equal to the measured roll damping at the natural frequency of oscillation in an extinction experiment; for other frequencies the increase is kept constant; the selection of the value of $q_{\phi\phi}$ is described in section 3;

c. as in b., but with $a_{y\phi} = a_{\phi y} = b_{y\phi} = b_{\phi y} = 0$; this does not mean that all coupling terms are zero, as $p_{y\phi} = p_{\phi y}$ and $q_{y\phi} = q_{\phi y}$ do not vanish because of the distance $\overline{OG}$;

d. according to the equation

$$\frac{\ddot{\phi}}{\omega_\phi^2} + \frac{\nu_\phi}{\omega_\phi}\dot{\phi} + \phi = \alpha_w e^{-kz_e} \tag{6}$$

presenting the usual formulation of pure rolling in beam waves; ω_ϕ and ν_ϕ are taken from the experiments; z_e is taken equal to $\frac{1}{2}T$.

3 Extinction experiments in roll and their analysis

The extinction experiments were done with the model located in the middle of the tank length and/or with the model close to the beach. The results show large differences, as will be seen. Assuming that the induced swaying can be neglected ($y = 0$) the test is described by equation (4) with $Y_w' = K_w' = 0$

$$p_{\phi\phi}\ddot{\phi} + q_{\phi\phi}\dot{\phi} + r_{\phi\phi}\phi = 0. \tag{7}$$

In equation (7) $r_{\phi\phi}$ is known: $r_{\phi\phi} = \varrho g A \cdot \overline{GM}$, while $p_{\phi\phi}$ can be approximated satisfactorily by measuring the natural period. Then $q_{\phi\phi}$ can be solved by recording the roll angle ϕ.

The natural period of the rolling is found to be

$$T_\phi = \frac{4\pi p_{\phi\phi}}{\sqrt{4p_{\phi\phi}r_{\phi\phi} - q_{\phi\phi}^2}} \tag{8}$$

For lightly damped oscillations (very small $q_{\phi\phi}$ compared to the product $p_{\phi\phi}r_{\phi\phi}$) this results for $p_{\phi\phi}$ in

$$p_{\phi\phi} \cong \frac{r_{\phi\phi}T_\phi^2}{4\pi^2} \tag{9}$$

From equation (5) it turns out that $p_{\phi\phi}$ is composed of many different contributions in which I, the mass-moment of inertia in air, will generally dominate the other terms. Yet equation (9) is thought to be a better approximation than $p_{\phi\phi} \cong I$, because it automatically takes into account the influence of the vertical position of G. Furthermore the relation (9) is much more practical since it is not easy to determine I.

The damping coefficient $q_{\phi\phi}$ is determined by the decrease of the oscillations, see figure 2. Putting

$$\delta = -\frac{q_{\phi\phi}}{2p_{\phi\phi}}T_\phi = \ln\phi_B - \ln\phi_A \tag{10}$$

it results in

$$q_{\phi\phi} = \left[\frac{r_{\phi\phi}p_{\phi\phi}\delta^2}{\pi^2 + \frac{1}{4}\delta^2}\right]^{\frac{1}{2}} \tag{11}$$

The measured T_ϕ and the experimental $q_{\phi\phi}$ are presented in figure 3 for condition 1 and in figure 4 for condition 2. For comparison the $b_{\phi\phi}$ and $q_{\phi\phi}$ given by potential theory are also indicated in the figures.

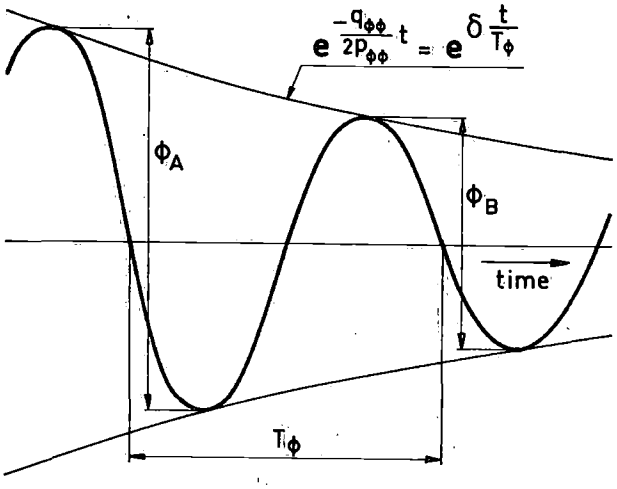

Fig. 2. Extinction curve for roll

It is to be expected that the actual roll damping during the tests is appreciably higher than a theoretical estimate because of the friction of the water film between the end bulkheads of the cylinder and the tank walls. The extinction experiments taken near the beach of the tank do not exhibit this tendency in figure 3. The curve B drawn through the 4 measured points intersects the theoretical $q_{\phi\phi}$-curve C. This must be due to reflection effects, but it cannot be explained further.

Unfortunately this fact was only established after the tests, while only 2 experiments in the middle of the

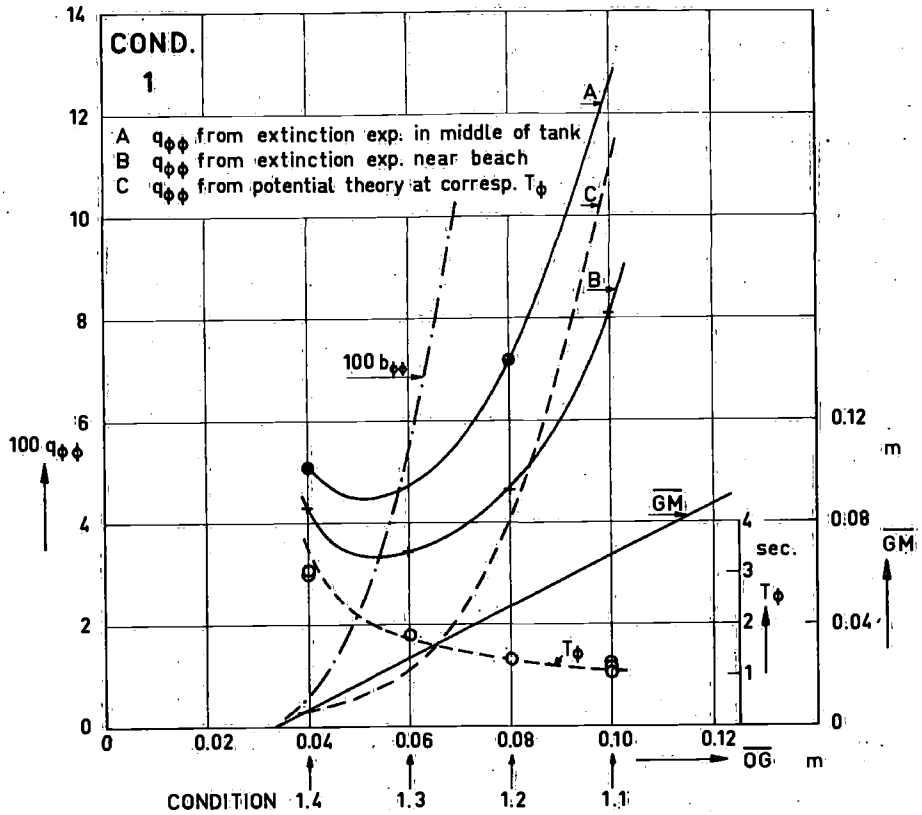

Fig. 3. Results of extinction experiments for condition 1

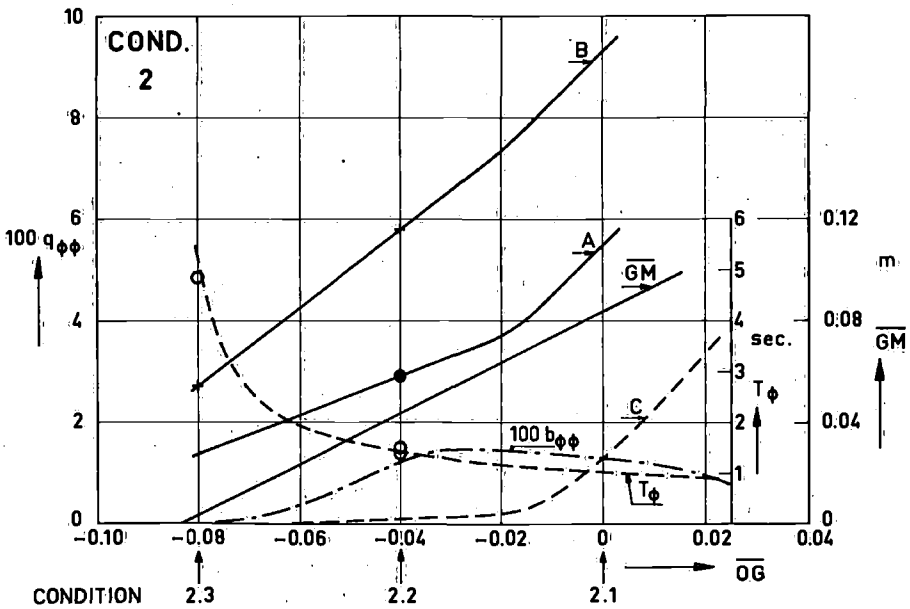

Fig. 4. Results of extinction experiments for condition 2

tank length were available. The ultimate $q_{\phi\phi}$-curve A, used in the motion predictions, is drawn through these two points and its trend has been adapted to curve B. Curve A does not intersect the theoretical curve C.

For condition 2 the same philosophy has been applied in figure 4. Here even fewer measurements were available, so that the $q_{\phi\phi}$-values are of a somewhat disputable nature. However, this has no serious consequences for the motion predictions.

It is remarkable that the mutual order of magnitude of the curves A and B in figure 4 is contrary to that in figure 3. An explanation cannot be given.

4 Experiments in regular waves

4.1 *The experimental set-up*

A sketch of the experimental facility is shown in figure 5. The wave generator is of the flap type. During the tests the point of rotation of the flap was at the tank bottom. The wave periods were varied between 0.5 sec and 2.4 sec. The wave height was kept constant at 0.02 m from crest to trough. The wave maker setting was determined before the actual tests without the model in the tank. The waves stated are therefore the undisturbed, incoming waves. However, it is possible that deviations from the nominal wave height occur since the generated waves will not be reproduced exactly.

The rolling was measured by a gyro installed in the cylinder. The accuracy of the measurements is approximately $\pm$ 0.2 degrees. For swaying a vertical rod was installed which hinged at the centre of gravity. It was connected to a very light cross which was guided horizontally. The motion of the cross was measured by a potentiometer, see figure 5. The accuracy of this set-up is about $\pm\ 0.2 \times 10^{-3}$ m.

Both roll angle and sway motion were recorded at a UV-recorder. The recordings showed a stationary part of sufficient length so that transient phenomena and later reflection and interference effects could be separated distinctly from the information desired.

The parts of the recordings mentioned were analysed manually to obtain the roll angle ϕ_a, sway amplitude y_a, the phase difference of sway with respect to roll $\varepsilon_{y\phi}$ and the drift velocity v. A typical example of a recording is reproduced in figure 6.

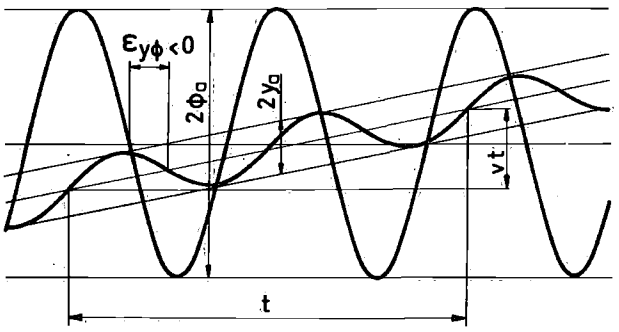

Fig. 6. Example of the experimental results

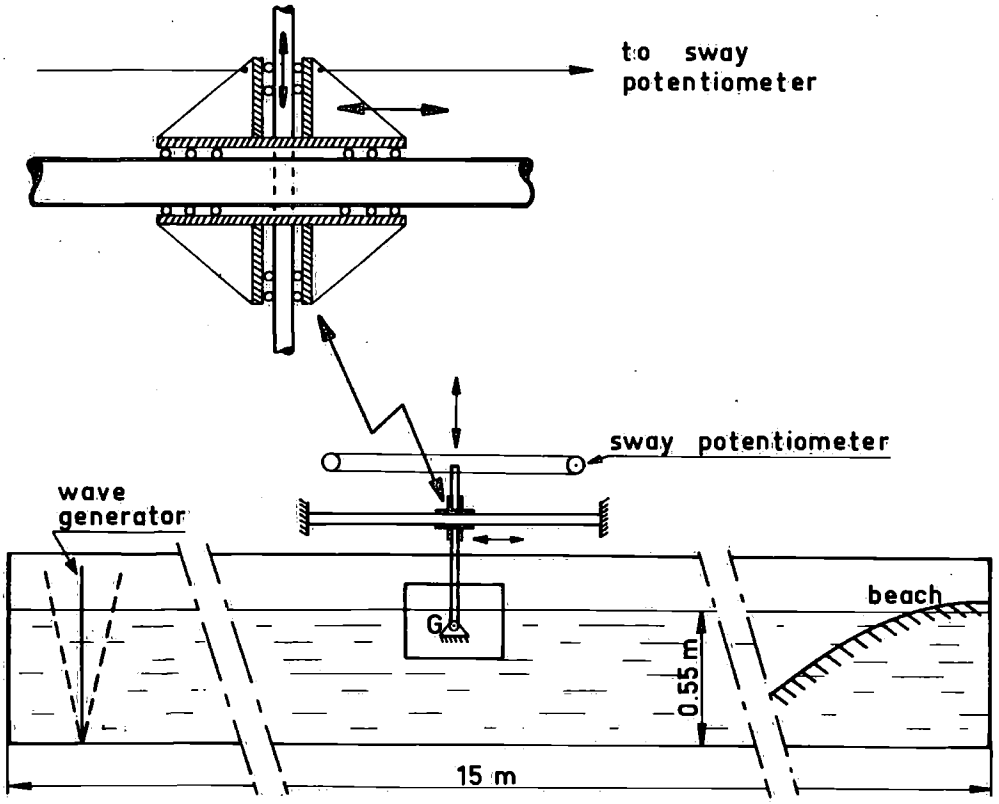

Fig. 5. Sketch of the experimental set-up

4.2 *The results of experiments and predictions*

The predicted heaving and its phase with respect to the wave motion at G is given in the figures 7 and 8. Heaving was not measured. By the finite water depth the motion of the water particles in the waves is deformed from a circle to an ellipse. The dotted line in the heave prediction is obtained by multiplication with the ratio (short axis ellipse at finite waterdepth)/ (diameter circle at infinite depth.)The ratio has been determined at a depth of the half draught of the section. This supposes that the dynamic performance of the cylinder can be separated from the static response and that the former is essentially unchanged. This seems a reasonable hypothesis for a first approximation.

The various $q_{\phi\phi}$-values used in the predictions a, b and c of section 2 are summarized in the figures A1 and A7 at the end of the paper. It is clear that the effect of the coupling coefficient $b_{\phi y}$ has a very great influence on $q_{\phi\phi}$ and cannot be neglected; compare the curves marked b and c, respectively.

The difference in the exciting moment used in the predictions a, b and c on the one hand and the Froude-Krylov moment in prediction d on the other hand is illustrated in the figures A2 and A8. It shows that the Froude-Krylov hypothesis is not a satisfactory base to compute the rolling moment.

The experimental results for rolling and swaying in condition 1 are presented in the figures A3 through A6. The four predictions according to section 2 are shown as well. The best theoretical prediction (curve b) for swaying has been multiplied with the ratio (long axis ellipse at finite waterdepth)/ (diameter circle at infinite depth) to account for the restricted waterdepth, just as in heaving.

The same information for condition 2 is given in the figures A9 through A11. An analogous correction for shallow water effects has been applied to swaying.

The measured drift velocities of both conditions have been plotted in figure A15 and A16.

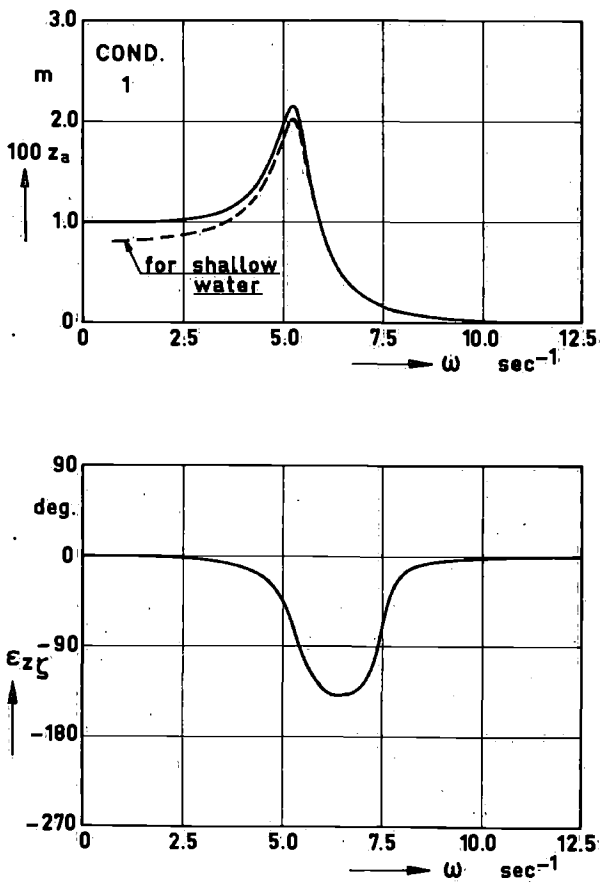

Fig. 7. Computed heaving for condition 1

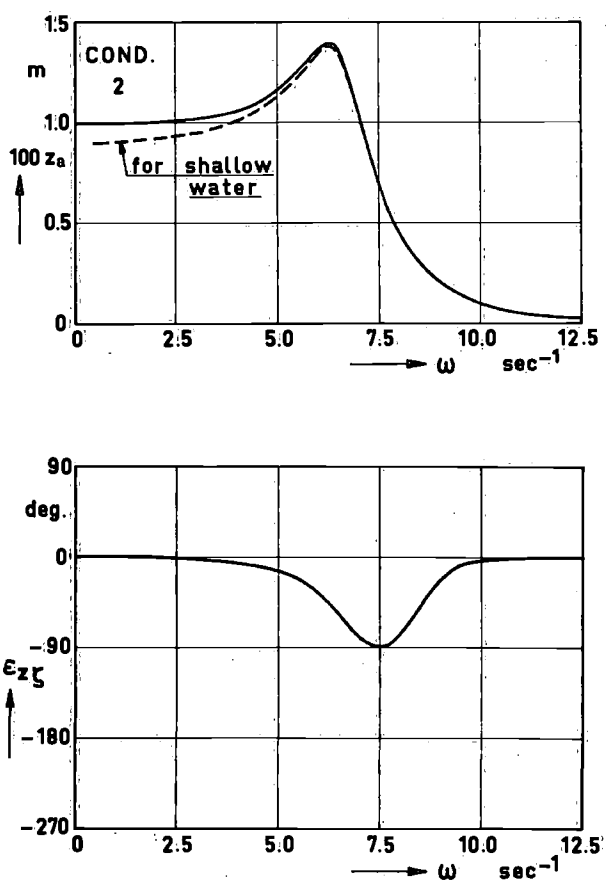

Fig. 8. Computed heaving for condition 2

5 Discussion of the results

The theoretical predictions, which are fundamentally most correct, are the curves marked b. The agreement between those curves and the experiments is generally very satisfactory. That the top of the roll resonance is lower or higher than the experiments is a direct consequence of the chosen value of $q_{\phi\phi}$, which could not be established very accurately, as discussed in section 3. The shift of the theoretical resonance zone with respect to the experimental resonance is of more fundamental interest, since it does not depend on $q_{\phi\phi}$. Yet it is not of great importance, considering the state of the art and possible practical applications. That the mathematical model is basically correct, is indicated clearly by the dip in the sway-curve and by the phase-relation $\varepsilon_{y\phi}$. The measurements of $\varepsilon_{y\phi}$ show an unexpected jump of about 180 degrees in some conditions, which is also found by the computations.

The completely theoretical curves, marked a, nearly coincide with the curves b, except for a narrow range about roll resonance. The increased roll damping lowers the ϕ_a-prediction, smooths the coupling effects of roll into sway and flattens the phase difference, but leaves the predictions further unchanged.

The same cannot be said about the curves marked c. It is clearly not a matter of accuracy but of the utmost importance to take due account of the coupling coefficients $a_{\phi y} = a_{y\phi}$ and $b_{\phi y} = b_{y\phi}$. This is most clearly demonstrated by the phase difference $\varepsilon_{y\phi}$, where the c-curves are distinctly in error. The greater the distance $\overline{OG}$ (positive for condition 1, or negative for condition 2) the greater their influence.

The predictions d, obtained by the familiar equation (6) for pure rolling in beam waves, differ in one case only slightly from the experiments (e.g. condition 1.2), in another case greatly. The general tendency of the coupling effects with swaying is to lower and to narrow the roll response, especially at the high frequency side. This can easily be shown by vector diagrams of the left-hand side of the roll equation of motion, using the computed $\varepsilon_{y\phi}$. This effect is particularly seen in condition 2.1 and 2.2. The phase lag $\varepsilon_{y\phi}$ does, of course, not show a jump of approximately 180 degrees as the predictions a and b and the experiments do in the conditions 1.4, 2.2 and 2.3. That the method d is not to be recommended for general use is also illustrated by condition 2.1. Here $\overline{OG} = 0$ so that for $a_{\phi y} = a_{y\phi} = b_{\phi y} = b_{y\phi} = 0$ rolling and swaying are fully decoupled. In principle now method c and d are equal, except for the precise value of $p_{\phi\phi}$ and $q_{\phi\phi}$ and determination of the exciting moment. These moments differ greatly, as is shown in figure A8. As a consequence the roll responses c and d differ also greatly; figure A9.

The exciting moment about G is composed of the hydrodynamic moment about O and the sway force

$$K_w = K'_w + \overline{OG} \cdot Y'_w.$$

K'_w and Y'_w are either in phase or in counterphase depending on the position of the metacentre M with respect to O. The distance $\overline{OG}$ may be positive or negative. Therefore K_w may become zero for a certain wave frequency and change in phase. This is shown in condition 2.2 at $\omega = 4.55$ sec^{-1}. In the conditions 1.4 and 2.3 the phase of K_w is contrary to that of the other conditions 1 and 2, respectively, for all frequencies.

It appears that the influence of shallow water on swaying can be accounted for reasonably by multiplication of the response with the ratio (long axis ellipse)/(diameter circle), given by the motion of the water particles in the wave at restricted and infinite depth. The experimental scatter is no doubt a consequence of wave reflection and subsequent interference effects, which were present for waves with periods longer than 1.5 sec. In the very low frequency range the measured roll angles generally show a slight hump. This must be attributed to a stronger coupling with swaying in the experiments by the much larger y_a-values than predicted. However, it is of no practical importance.

Finally the theoretical results marked b for condition 1 and for condition 2 have been plotted non-dimensionally in figure A12 en A13, using $\overline{GM}/B$ as a parameter. The base of these figures is ω/ω_{res}, where ω_{res} is the frequency where the largest ϕ_a is found in the respective curves labelled b. The figures exhibit some interesting features. Rolling is a typical resonance phenomenon. When plotted on the basis of tuning factor the curves nearly coincide. There is a very narrow peak, which has a slight tendency to become somewhat broader when the $\overline{GM}$ decreases. Little can be said about the maximum magnification factor for the various conditions 1 or 2 separately. But for condition 1 as a whole it is roughly twice as large as for condition 2. This is not explained by the nondimensional damping coefficients $Q = q_{\phi\phi}/\sqrt{p_{\phi\phi} r_{\phi\phi}}$ which have been plotted in figure A14. Q is equivalent to v_ϕ for the one degree of freedom rolling. But contrary to v_ϕ Q does not solely control the rolling at resonance by the coupling effects.

Swaying on the other hand is an absolute phenomenon mainly dependent on the waves. Plotted on wave frequency the curves for the various conditions 1 practically coincide (figures A3–A6), just as for the conditions 2 (figures A9–A11). Only at roll resonance there is a different performance by coupling. On a basis of roll tuning factor the various sway curves are

distinctly different (figures A12 and A13). The influence of the coupling effects, causing the hump and hollow in the sway curves, decreases strongly, when $\overline{GM}$ decreases. Both the magnitude and the width of the influenced range become less.

The phase difference $\varepsilon_{y\phi}$ is a relative quantity, just as rolling. For condition 1 $\varepsilon_{y\phi}$ varies somewhat with $\overline{GM}/B$, for condition 2 hardly any difference can be noticed.

During the tests the drift velocities have been measured. The fact that there is a drift velocity shows that apart from the oscillatory lateral force a mean component must be present. No attempt has been made to predict or to analyse this effect, but the experimental results are shown in the figures A15 and A16. It is not impossible that especially these secondary effects are strongly influenced by the test circumstances as the way of generating waves and the dimensions of the tank. So the information must be used carefully.

6 Conclusions

1. The experiments show that the mathematical model of section 2 is fundamentally correct. Roll and sway are coupled by comprehensive coefficients made up of the actual coupling coefficients $a_{\phi y}$ and $b_{\phi y}$, of the hydrodynamic sway coefficients a_{yy} and b_{yy} and of the vertical position of the centre of gravity $\overline{OG}$.
2. Taking the coupling coefficients $a_{\phi y}$ and $b_{\phi y}$ into account is not a matter of improving the accuracy, but of primary importance for the mathematical model to exhibit the essential characteristics of the phenomena. Compare the curves labelled b and c in the figures A3–A6 and A9–A11.
3. Increasing the roll damping does not introduce any new aspect in the motions; it solely lowers the peak value in rolling, flattens the hump and hollow in the sway-curve at roll resonance and makes the phase transition less steep. See the curves a and b in the figures A3–A6 and A9–A11.
4. In general the Froude-Krylov moment cannot be considered as a sound base for the excitation in rolling. See figure A2 and A8. The actual moment is not only dependent on the metacentric height, so on the relative position of G and M, but also on the absolute position of G and M with respect to the water surface.
5. The one degree of freedom prediction (curves d in the figures A3–A6 and A9–A11) sometimes offers reasonable results, sometimes the results are poor. It is better to use an advanced method of prediction, which takes the important variables into account.
6. The influence of the coupling of roll into sway is not large; see figure A12 and A13. The influence still decreases for diminishing $\overline{GM}$. The influence of the coupling of sway into roll cannot be estimated beforehand. It will depend on the shape of the section, the condition of loading and the vertical position of the centre of gravity. So it may be quite different in different cases. The general tendency is to lower and to narrow the roll response, especially at the high frequency side.
7. For the various sub-conditions the relative roll response is very similar, both to magnitude and phase, despite the large differences in $\overline{GM}/B$. See figure A12 and A13.
8. The shallow water effect on swaying is very reasonably accounted for by multiplication of the deep water response with the ratio (long axis ellipse) /(diameter circle) of the track of the water particles in the wave.

Acknowledgement

The experiments described in this report have been carried out for the author by the American students O. H. Oakley of M.I.T. and P. B. Fontneau of Webb Institute in July 1967, during their stay at the Shipbuilding Laboratory as student-trainees. The author expresses his sincere gratitude for their work.

References

1. Tasai, F., Ship motions in beam seas. Reports of Research Institute for Applied Mechanics Kyushu University, Vol. XIII, No. 45, 1965.
2. Vugts, J. H., The hydrodynamic coefficients for swaying, heaving and rolling cylinders in a free surface. Netherlands Ship Research Centre TNO, Report 112 S, May 1968.

APPENDIX

PRESENTATION OF THE RESULTS

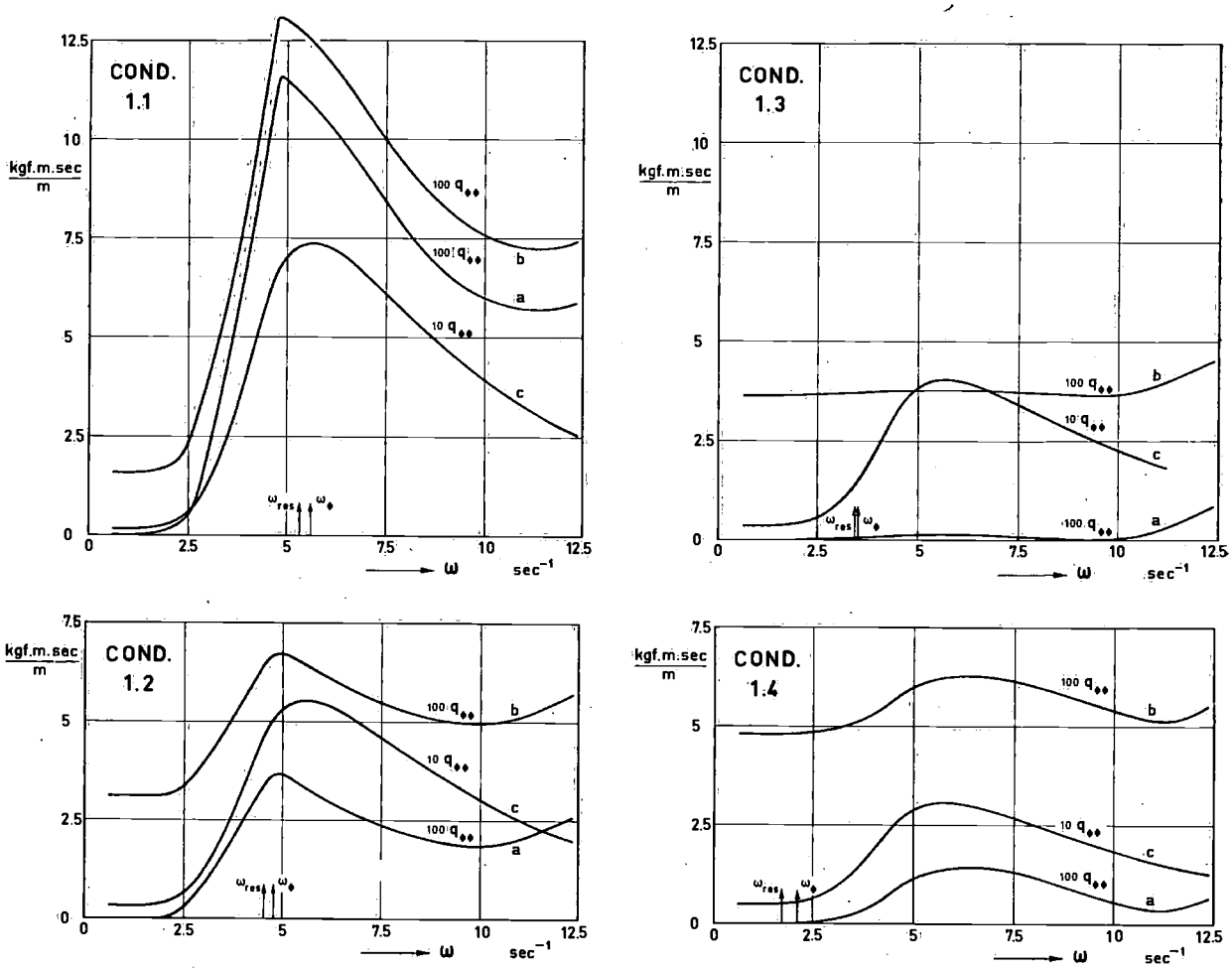

Fig. A1. Computed values of the roll damping coefficient for the predictions a, b and c; condition 1

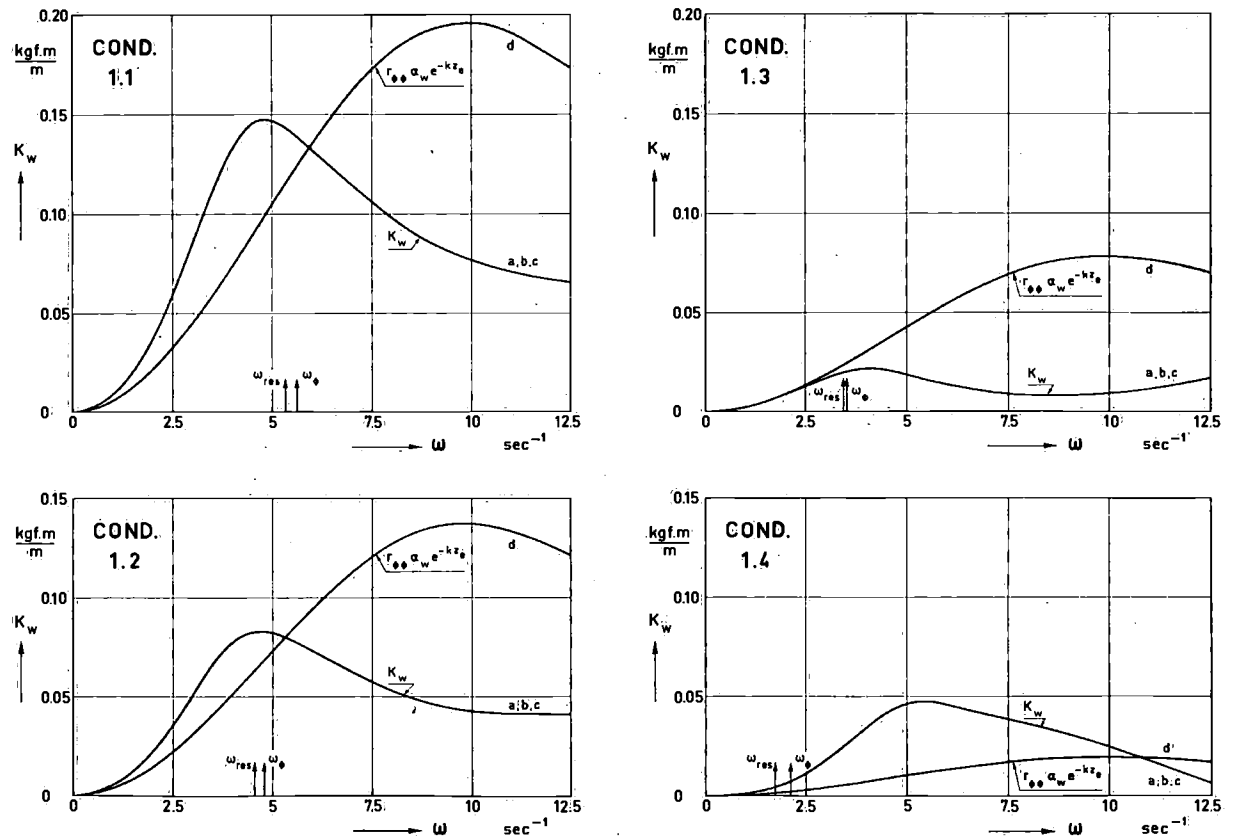

Fig. A2. Comparison of the computed wave exciting moment and the Froude-Krylov moment; condition 1

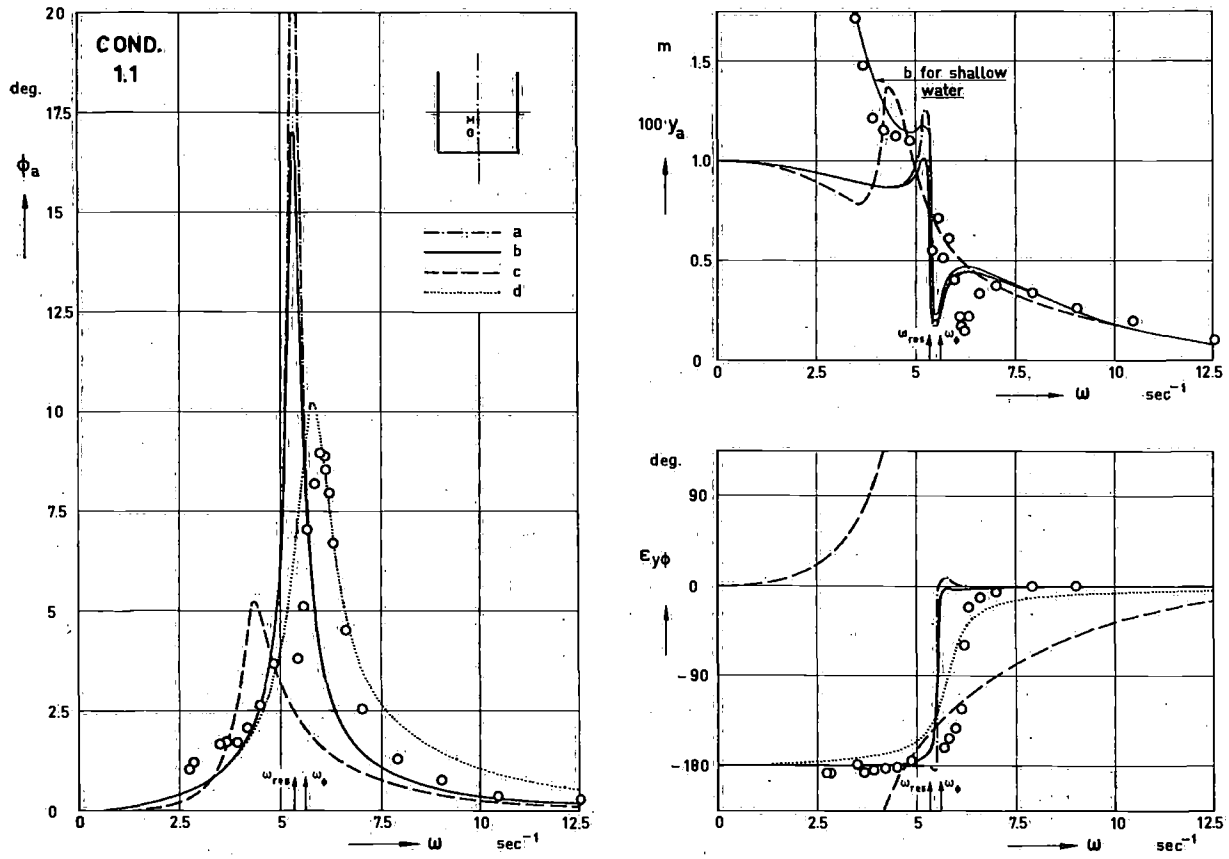

Fig. A3. Rolling and swaying for condition 1.1

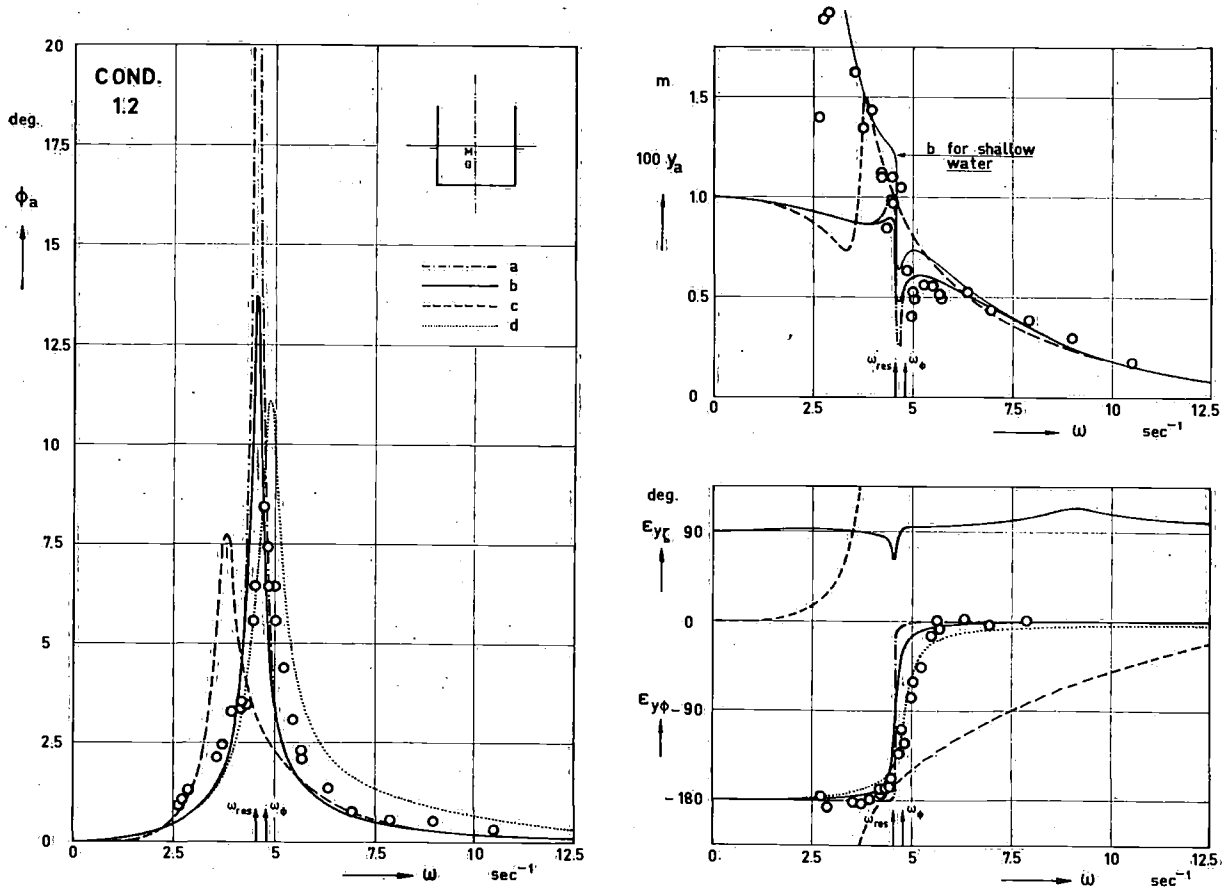

Fig. A4. Rolling and swaying for condition 1.2

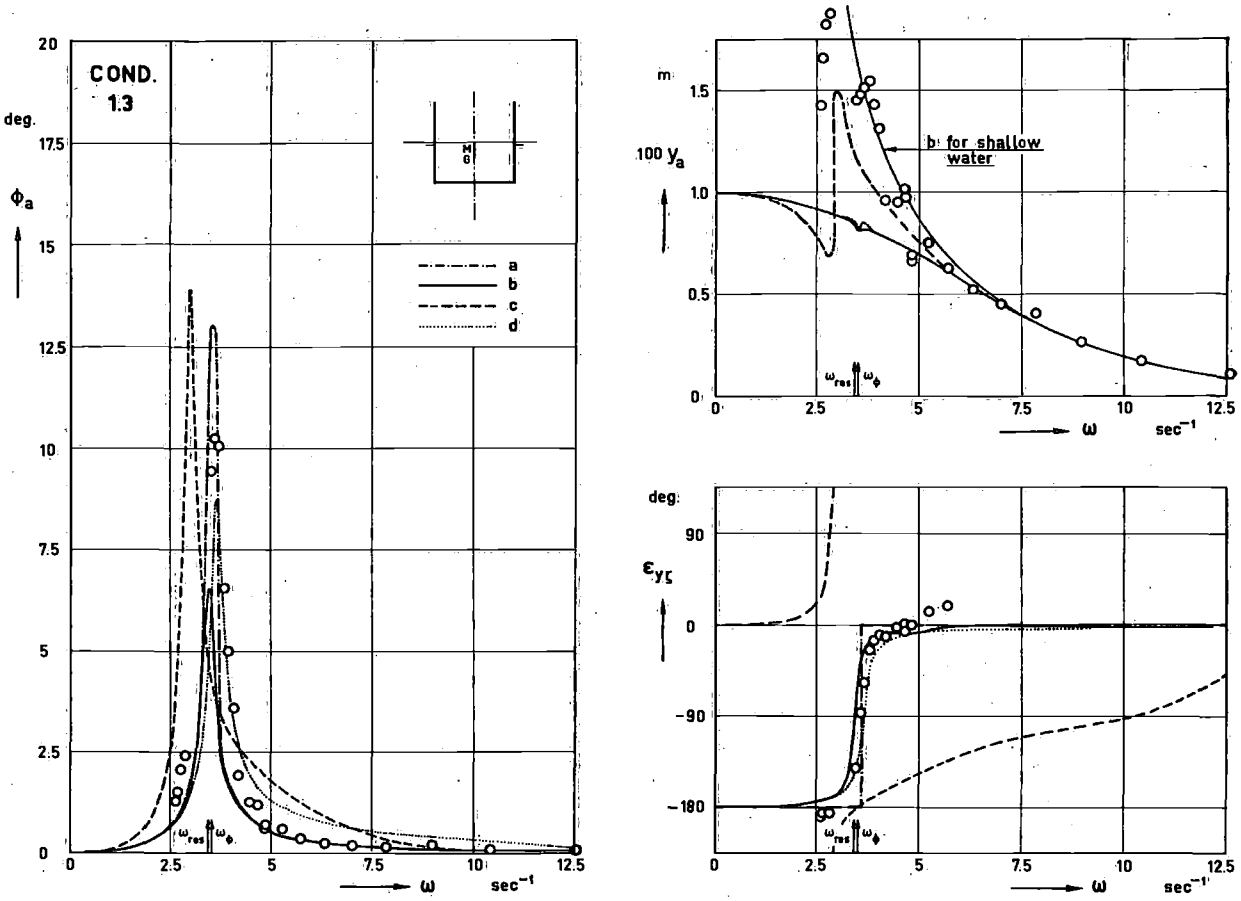

Fig. A5. Rolling and swaying for condition 1.3

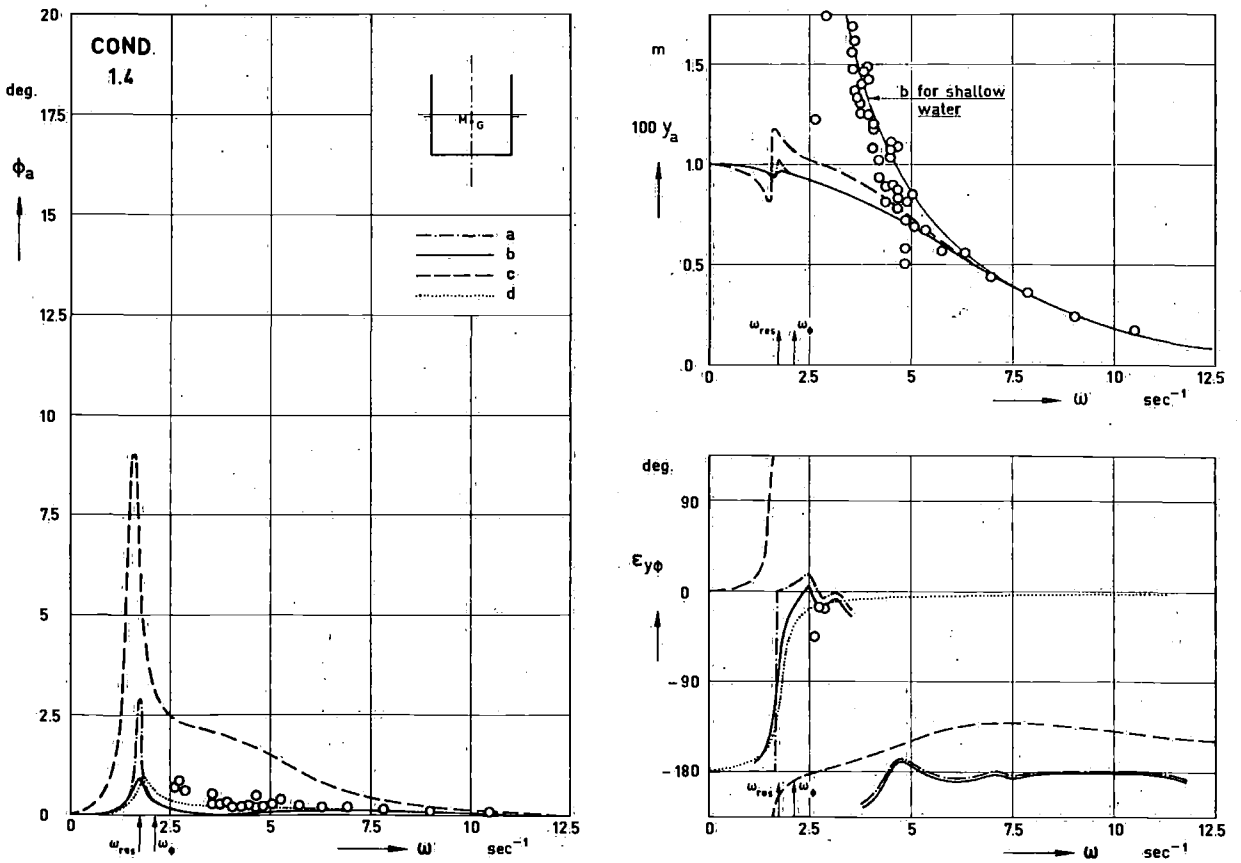

Fig. A6. Rolling and swaying for condition 1.4

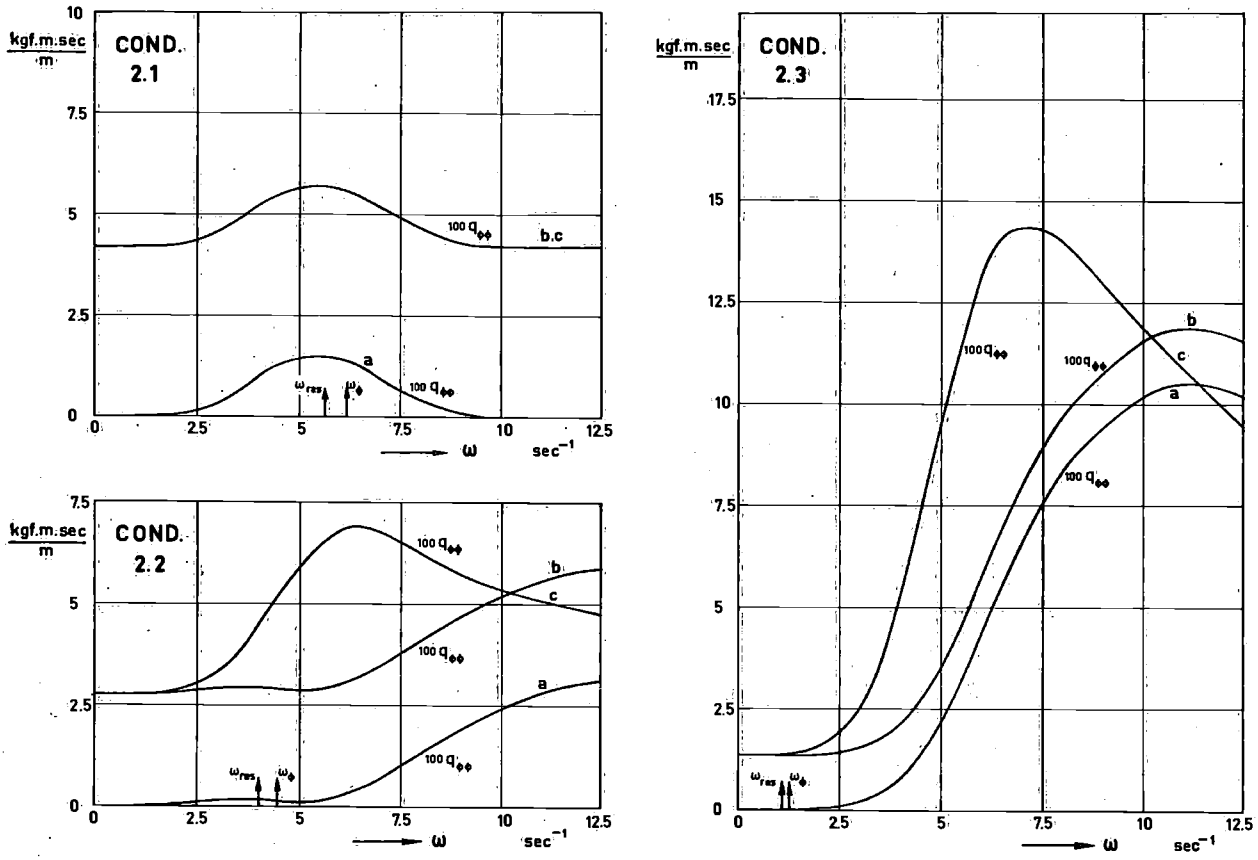

Fig. A7. Computed values of the roll damping coefficient for the predictions a, b and c; condition 2

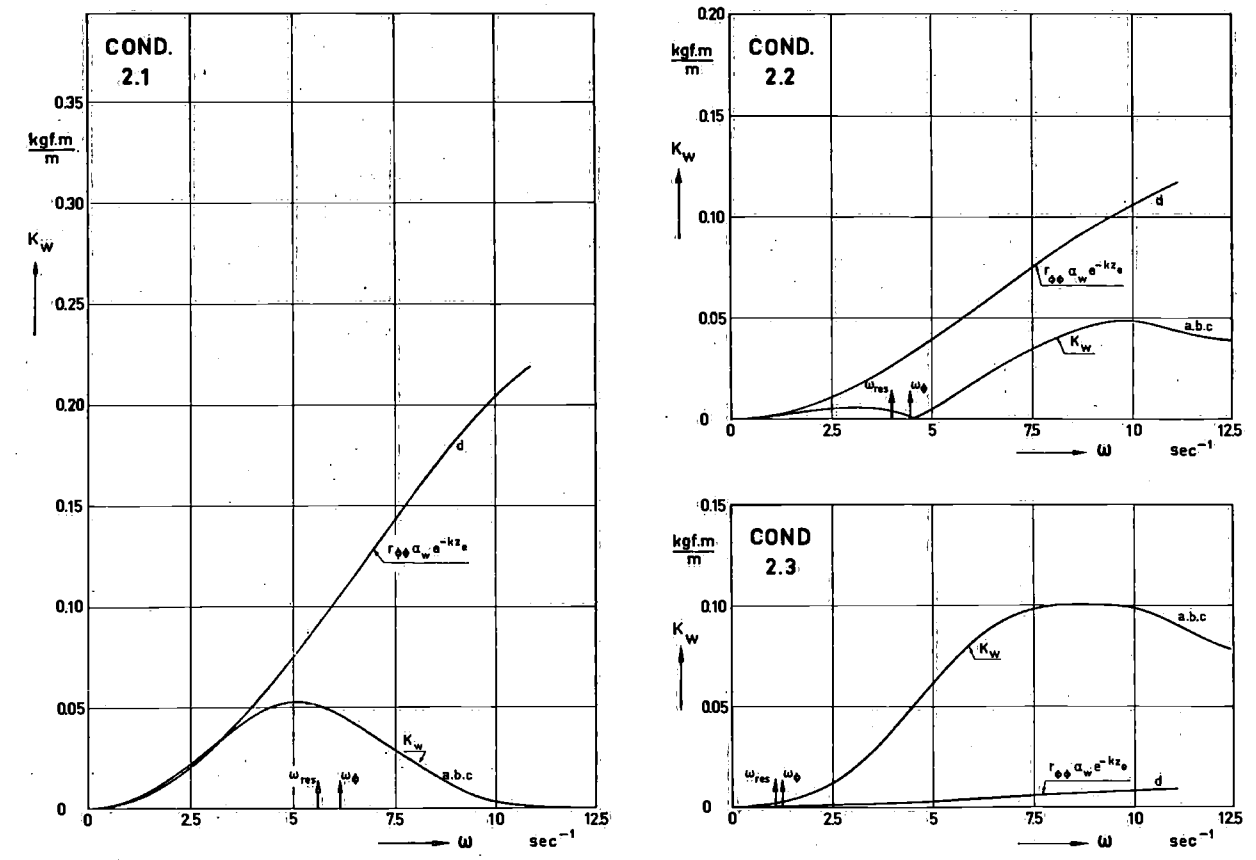

Fig. A8. Comparison of the computed wave exciting moment and the Froude-Krylov moment; condition 2

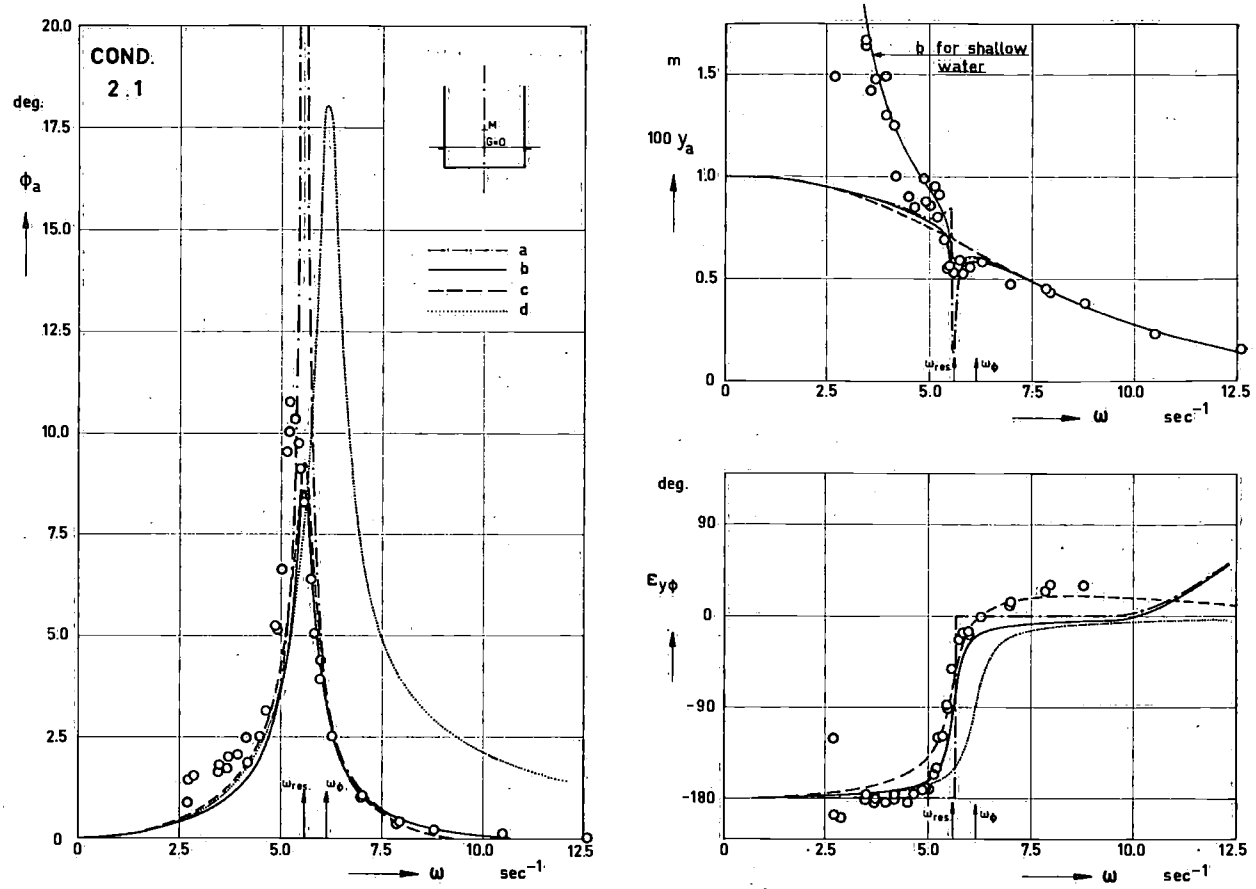

Fig. A9. Rolling and swaying for condition 2.1

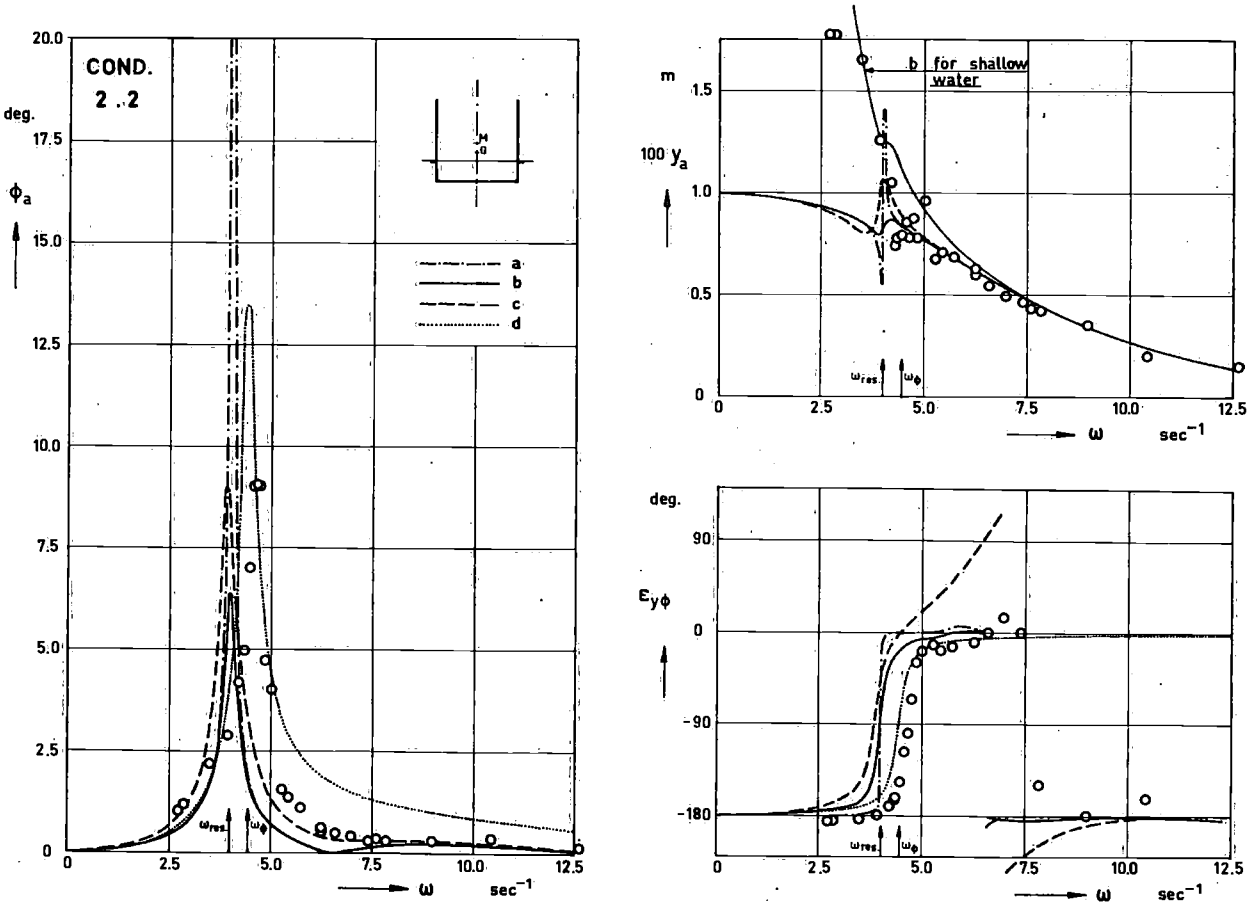

Fig. A10. Rolling and swaying for condition 2.2

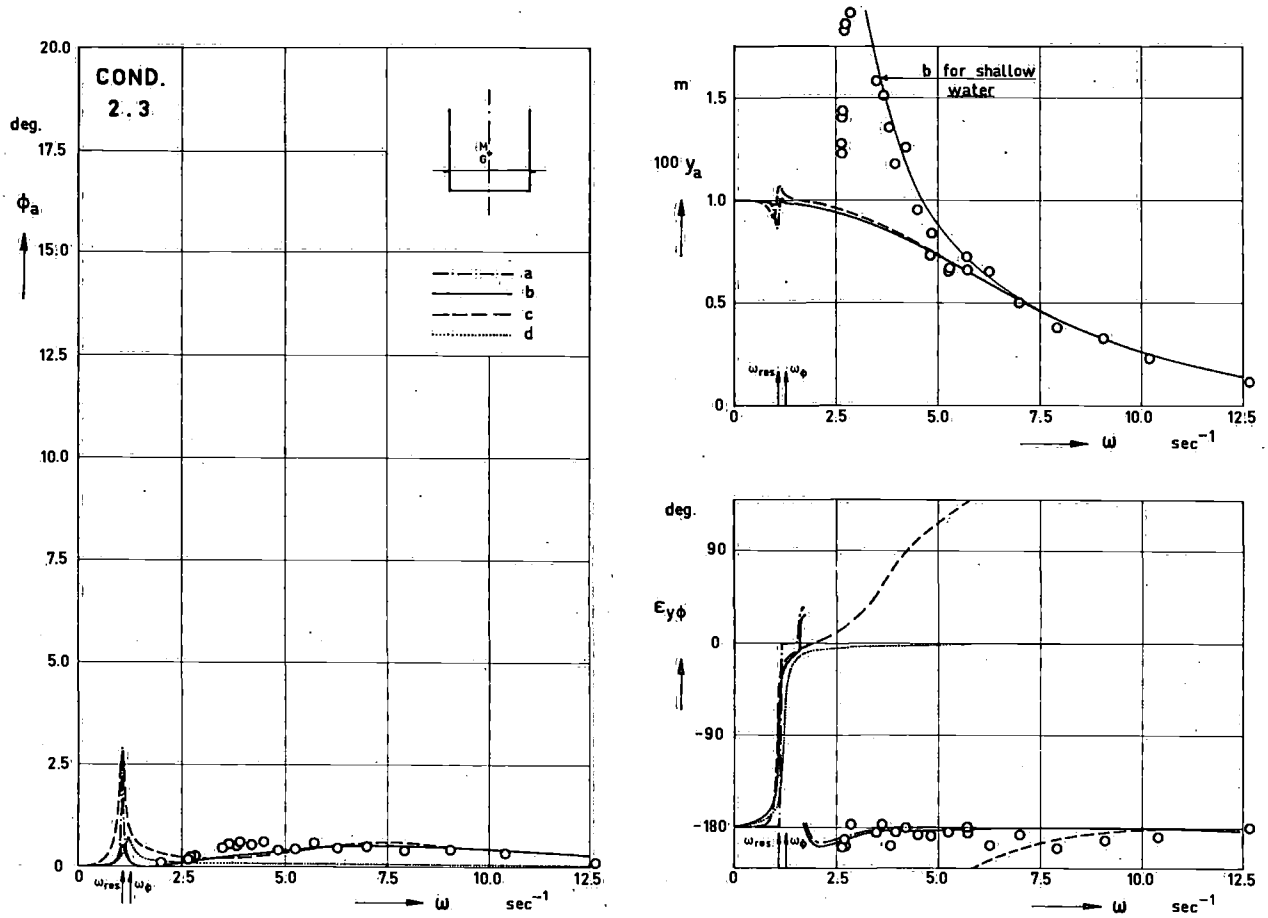

Fig. A11. Rolling and swaying for condition 2.3

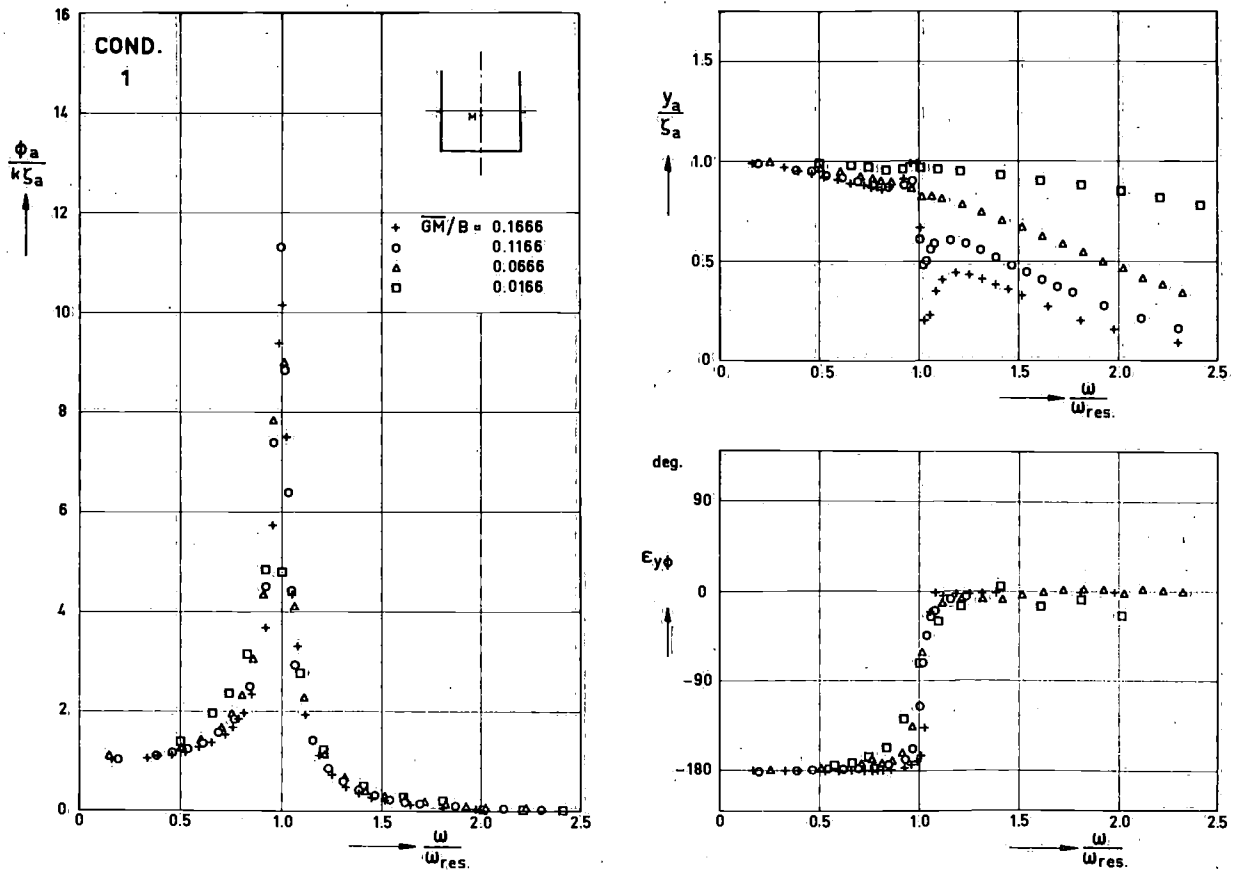

Fig. A12. Nondimensional rolling and swaying for condition 1

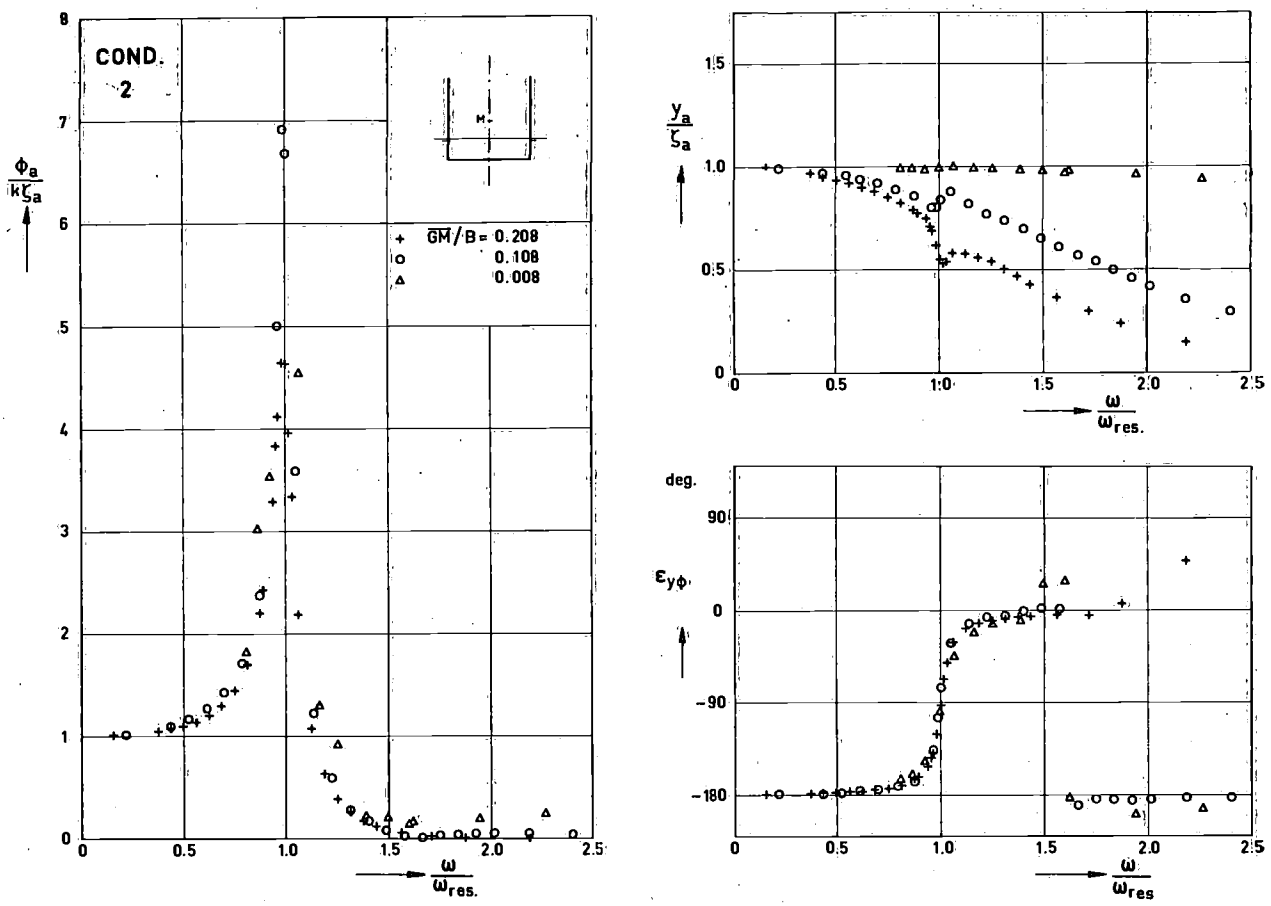

Fig. A13. Nondimensional rolling and swaying for condition 2

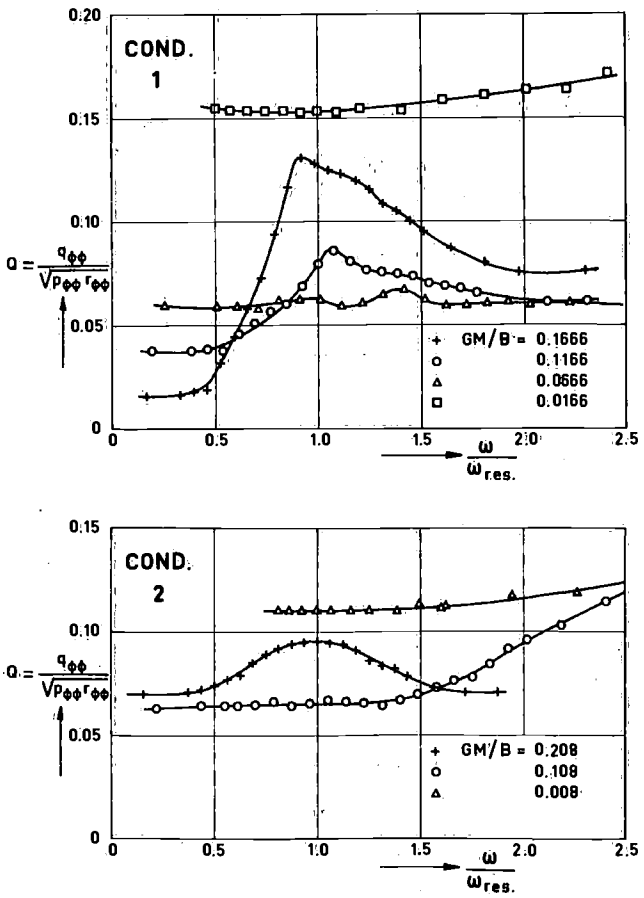

Fig. A14. Nondimensional roll damping coefficients

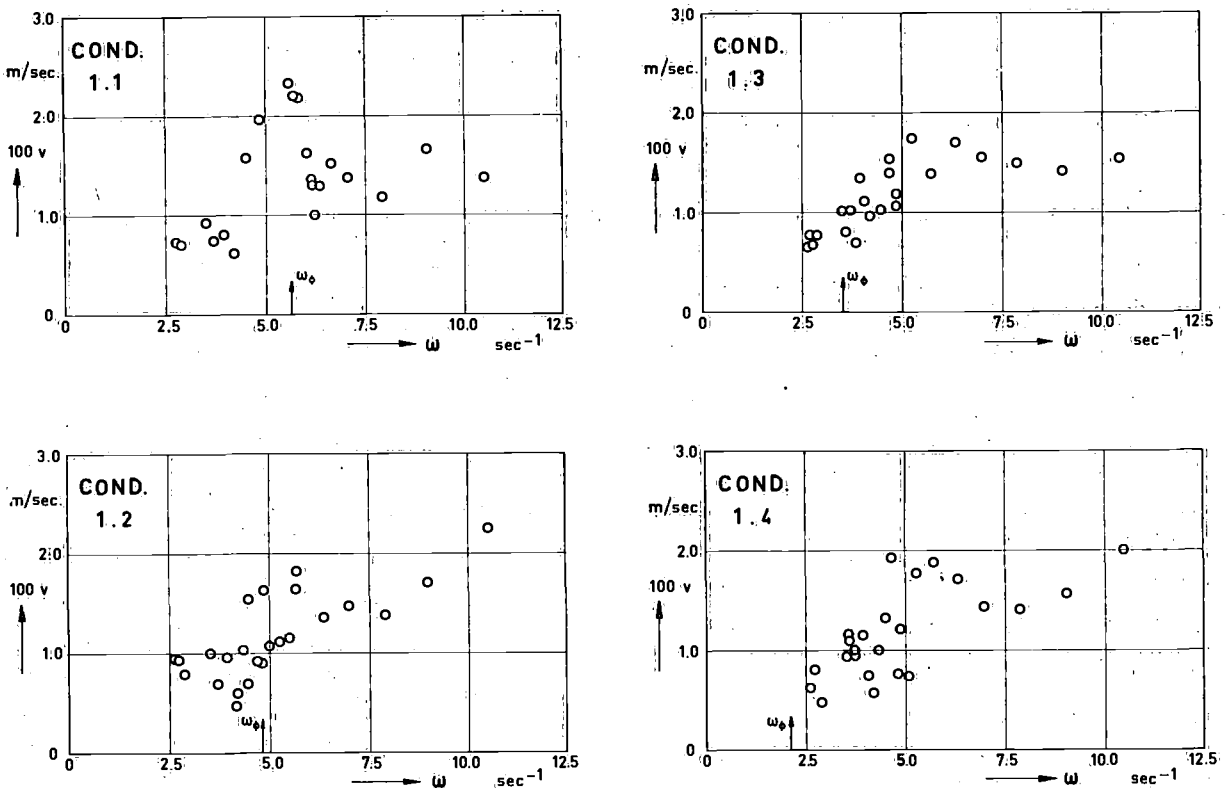

Fig. A15. Measured drift velocities for condition 1

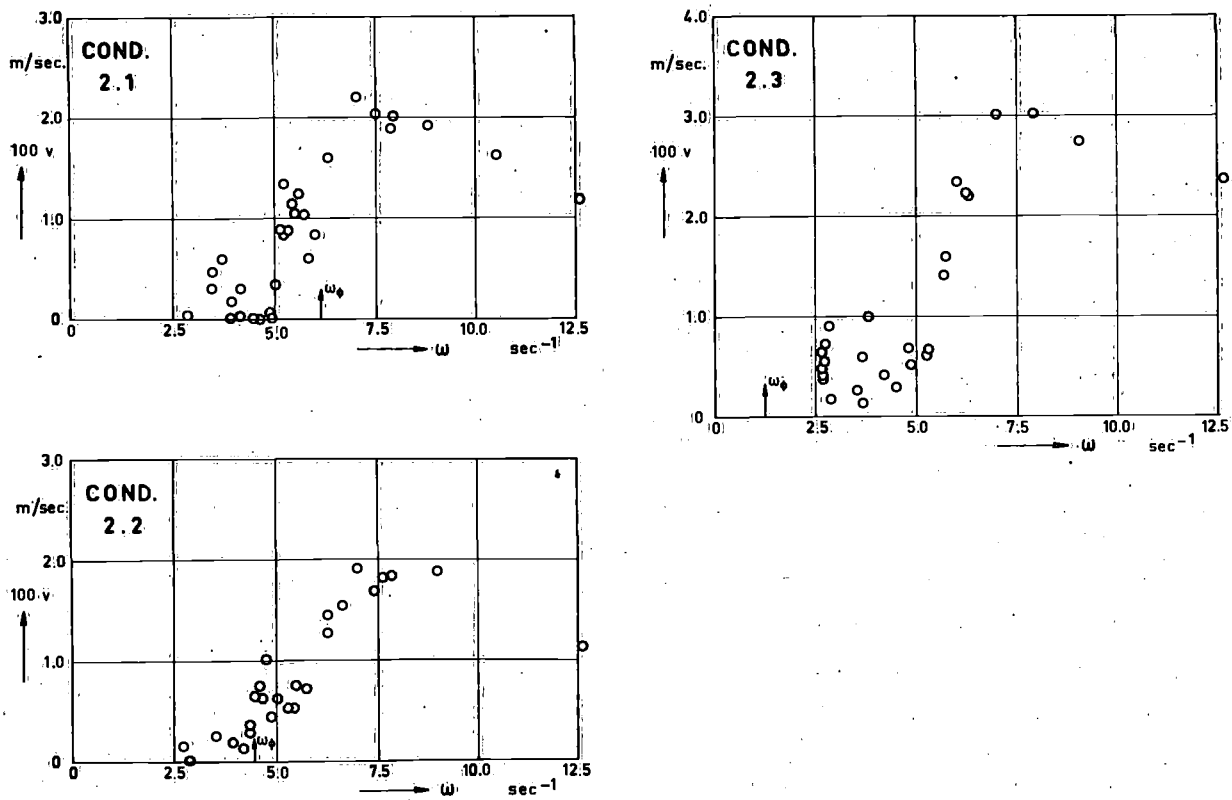

Fig. A16. Measured drift velocities for condition 2

PUBLICATIONS OF THE NETHERLANDS SHIP RESEARCH CENTRE TNO

PUBLISHED AFTER 1963 (LIST OF EARLIER PUBLICATIONS AVAILABLE ON REQUEST)
PRICE PER COPY DFL. 10,—

M = engineering department S = shipbuilding department C = corrosion and antifouling department

Reports

57 M Determination of the dynamic properties and propeller excited vibrations of a special ship stern arrangement. R. Wereldsma, 1964.
58 S Numerical calculation of vertical hull vibrations of ships by discretizing the vibration system, J. de Vries, 1964.
59 M Controllable pitch propellers, their suitability and economy for large sea-going ships propelled by conventional, directly coupled engines. C. Kapsenberg, 1964.
60 S Natural frequencies of free vertical ship vibrations. C. B. Vreugdenhil, 1964.
61 S The distribution of the hydrodynamic forces on a heaving and pitching shipmodel in still water. J. Gerritsma and W. Beukelman, 1964.
62 C The mode of action of anti-fouling paints: Interaction between anti-fouling paints and sea water. A. M. van Londen, 1964.
63 M Corrosion in exhaust driven turbochargers on marine diesel engines using heavy fuels. R. W. Stuart Michell and V. A. Ogale, 1965.
64 C Barnacle fouling on aged anti-fouling paints; a survey of pertinent literature and some recent observations. P. de Wolf, 1964.
65 S The lateral damping and added mass of a horizontally oscillating shipmodel. G. van Leeuwen, 1964.
66 S Investigations into the strength of ships' derricks. Part. I. F. X. P. Soejadi, 1965.
67 S Heat-transfer in cargotanks of a 50,000 DWT tanker. D. J. van der Heeden and L. L. Mulder, 1965.
68 M Guide to the application of Method for calculation of cylinder liner temperatures in diesel engines. H. W. van Tijen, 1965.
69 M Stress measurements on a propeller model for a 42,000 DWT tanker. R. Wereldsma, 1965.
70 M Experiments on vibrating propeller models. R. Wereldsma, 1965.
71 S Research on bulbous bow ships. Part II. A. Still water performance of a 24,000 DWT bulkcarrier with a large bulbous bow. W. P. A. van Lammeren and J. J. Muntjewerf, 1965.
72 S Research on bulbous bow ships. Part. II. B. Behaviour of a 24,000 DWT bulkcarrier with a large bulbous bow in a seaway. W. P. A. van Lammeren and F. V. A. Pangalila, 1965.
73 S Stress and strain distribution in a vertically corrugated bulkhead. H. E. Jaeger and P. A. van Katwijk, 1965.
74 S Research on bulbous bow ships. Part. I. A. Still water investigations into bulbous bow forms for a fast cargo liner. W. P. A. van Lammeren and R. Wahab, 1965.
75 S Hull vibrations of the cargo-passenger motor ship "Oranje Nassau", W. van Horssen, 1965.
76 S Research on bulbous bow ships. Part I. B. The behaviour of a fast cargo liner with a conventional and with a bulbous bow in a seaway. R. Wahab, 1965.
77 M Comparative shipboard measurements of surface temperatures and surface corrosion in air cooled and water cooled turbine outlet casings of exhaust driven marine diesel engine turbochargers. R. W. Stuart Mitchell and V. A. Ogale, 1965.
78 M Stern tube vibration measurements of a cargo ship with special afterbody. R. Wereldsma, 1965.
79 C The pre-treatment of ship plates: A comparative investigation on some pre-treatment methods in use in the shipbuilding industry. A. M. van Londen, 1965.
80 C The pre-treatment of ship plates: A practical investigation into the influence of different working procedures in over-coating zinc rich epoxy-resin based pre-construction primers. A. M. van Londen and W. Mulder, 1965.
81 S The performance of U-tanks as a passive anti-rolling device. C. Stigter, 1966.
82 S Low-cycle fatigue of steel structures. J. J. W. Nibbering and J. van Lint, 1966.
83 S Roll damping by free surface tanks. J. J. van den Bosch and J. H. Vugts, 1966.
84 S Behaviour of a ship in a seaway, J. Gerritsma, 1966.
85 S Brittle fracture of full scale structures damaged by fatigue. J. J. W. Nibbering, J. van Lint and R. T. van Leeuwen, 1966.
86 M Theoretical evaluation of heat transfer in dry cargo ship's tanks using thermal oil as a heat transfer medium. D. J. van der Heeden, 1966.
87 S Model experiments on sound transmission from engineroom to accommodation in motorships. J. H. Janssen, 1966.
88 S Pitch and heave with fixed and controlled bow fins. J. H. Vugts, 1966.
89 S Estimation of the natural frequencies of a ship's double bottom by means of a sandwich theory. S. Hylarides, 1967.
90 S Computation of pitch and heave motions for arbitrary ship forms. W. E. Smith, 1967.
91 M Corrosion in exhaust driven turbochargers on marine diesel engines using heavy fuels. R. W. Stuart Mitchell, A. J. M. S. van Montfoort and V. A. Ogale, 1967.
92 M Residual fuel treatment on board ship. Part II. Comparative cylinder wear measurements on a laboratory diesel engine using filtered or centrifuged residual fuel. A. de Mooy, M. Verwoest and G. G. van der Meulen, 1967.
93 C Cost relations of the treatments of ship hulls and the fuel consumption of ships. H. J. Lageveen-van Kuijk, 1967.
94 C Optimum conditions for blast cleaning of steel plate. J. Remme' 1967.
95 M Residual fuel treatment on board ship. Part. I. The effect of centrifuging, filtering and homogenizing on the unsolubles in residual fuel. M. Verwoest and F. J. Colon, 1967.
96 S Analysis of the modified strip theory for the calculation of ship motions and wave bending moments. J. Gerritsma and W. Beukelman, 1967.
97 S On the efficacy of two different roll-damping tanks. J. Bootsma and J. J. van den Bosch, 1967.
98 S Equation of motion coefficients for a pitching and heaving destroyer model. W. E. Smith, 1967.
99 S The manoeuvrability of ships on a straight course. J. P. Hooft, 1967.
100 S Amidships forces and moments on a $C_B = 0.80$ "Series 60" model in waves from various directions. R. Wahab, 1967.
101 C Optimum conditions for blast cleaning of steel plate. Conclusion. J. Remmelts, 1967.
102 M The axial stiffness of marine diesel engine crankshafts. Part I. Comparison between the results of full scale measurements and those of calculations according to published formulae. N. J. Visser, 1967.
103 M The axial stiffness of marine diesel engine crankshafts. Part II. Theory and results of scale model measurements and comparison with published formulae. C. A. M. van der Linden, 1967.
104 M Marine diesel engine exhaust noise. Part I. A mathematical model. J. H. Janssen, 1967.
105 M Marine diesel engine exhaust noise. Part II. Scale models exhaust systems. J. Buiten and J. H. Janssen, 1968.
106 M Marine diesel engine exhaust noise. Part. III. Exhaust sound criteria for bridge wings. J. H. Janssen en J. Buiten. 1967.
107 S Ship vibration analysis by finite element technique. Part. I. General review and application to simple structures, statically loaded. S. Hylarides, 1967.
108 M Marine refrigeration engineering. Part I. Testing of a decentralised refrigerating installation. J. A. Knobbout and R. W. J. Kouffeld, 1967.
109 S A comparative study on four different passive roll damping tanks. Part I. J. H. Vugts, 1968.
110 S Strain, stress and flexure of two corrugated and one plane bulkhead subjected to a lateral, distributed load. H. E. Jaeger and P. A. van Katwijk, 1968.
111 M Experimental evaluation of heat transfer in a dry-cargo ships' tank, using thermal oil as a heat transfer medium. D. J. van der Heeden, 1968.
112 S The hydrodynamic coefficients for swaying, heaving and rolling cylinders in a free surface. J. H. Vugts, 1968.
113 M Marine refrigeration engineering Part II. Some results of testing a decentralised marine refrigerating unit with R 502. J. A. Knobbout and C. B. Colenbrander, 1968.
115 S Cylinder motions in beam waves. J. H. Vugts, 1968.
116 M Torsional-axial vibrations of a ship's propulsion system. Part I. Comparative investigation of calculated and measured torsional-axial vibrations in the shafting of a dry cargo motorship. C. A. M. van der Linden, H. H. 't Hart and E. R. Dolfin, 1968.